Data Input to Hadronic Vacuum Polarisation

Zhiqing ZHANG

Outline of the lecture

1. Introduction
2. Inputs
3. Data combination
4. Results and discussions
5. Summary and perspectives

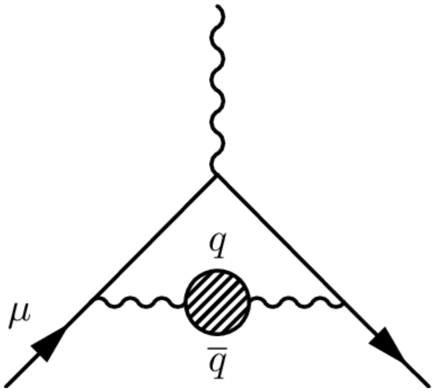

HVP
Hadronic Vacuum Polarisation

Situation in 2021

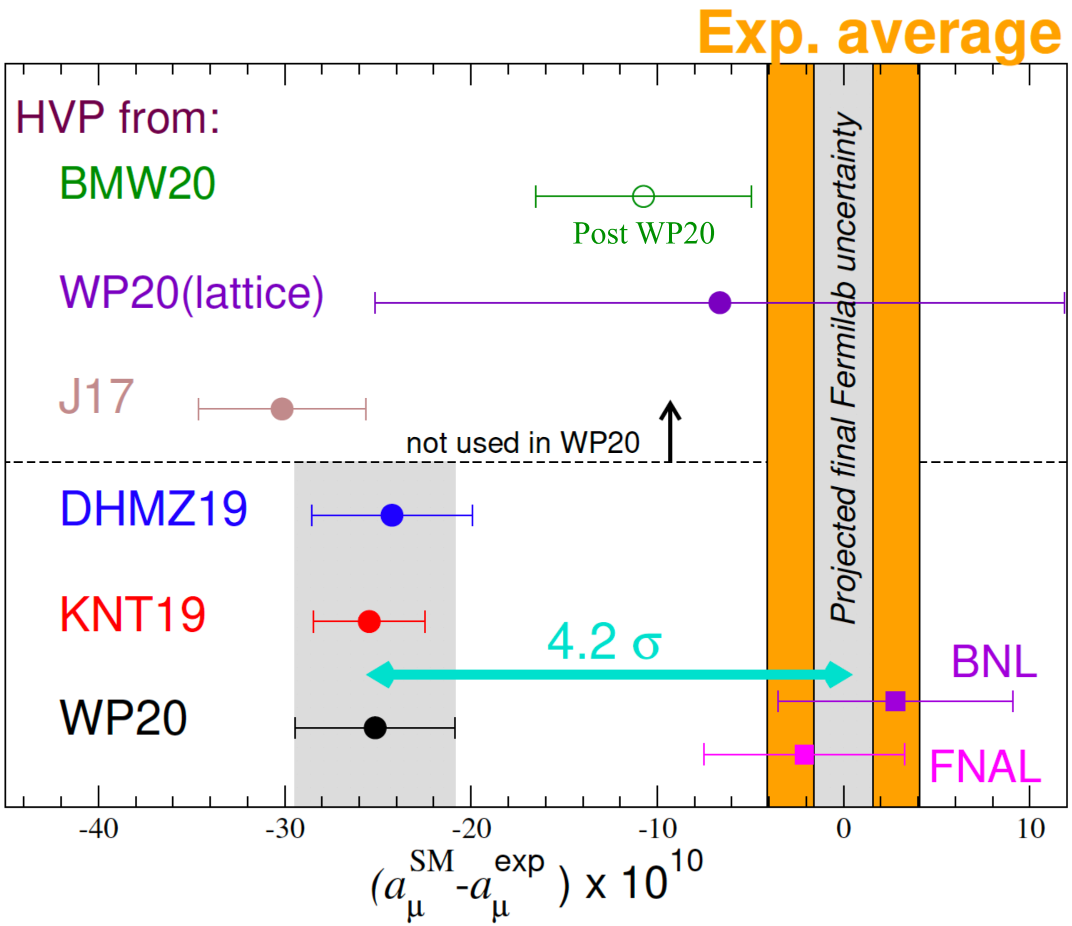

WP20: White Paper published in 2020
Phys. Rep. 887 (2020) 1

An outcome after several dedicated workshops since 2017

In the following, I shall discuss the input to the HVP calculation, take mainly DHMZ19 as an example

A discrepancy of 4.2σ
→ Strong evidence for new physics?

DHMZ19

Component	All numbers in units of 10^{-10}	Reference
QED	11 658 471.895 (0.008)	Aoyama-Hayakawa-Kinoshita-Nio, PRL 109, 111808 (2012)
EW	15.36 (0.10)	Gnendiger-Stökinger-Stökinger-Kim, PRD 88, 053005 (2013)
HVP LO	694.0 (4.0)	Davier-Hoecker-Malaescu-Zhang, EPJC 80, 241 (2020)
HVP NLO HVP NNLO	−9.87 (0.09) 1.24 (0.01)	Kurz-Liu-Marquard-Steinhauser, PLB 734, 144 (2014)
HVP LBL	10.5 (2.6)	Prades-de Rafael-Vainshtein, Ser. Direct. HEP 20, 303 (2009)
Total	11 659 183.1 (4.0) (2.6) (0.1)	

The uncertainty is dominated by the HVP LO contribution

➔ The focus of the study and discussion

LO HVP Calculation

The LO HVP contribution can be expressed in terms of two-point correlation function or hadronic vacuum polarisation tensor

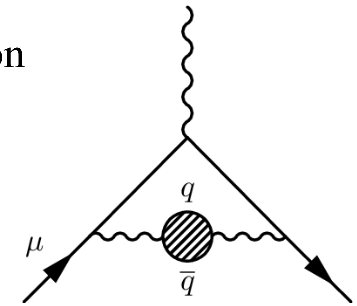

$$a_\mu^{\mathrm{HVP}} = 4\alpha^2 \int_0^\infty dQ^2 f(Q^2)\Pi(Q^2)$$

$$\Pi_{\mu\nu}(Q^2) = \int d^4x e^{iQx}\langle J_\mu(x)J_\nu(0)\rangle = \left(Q_\mu Q_\nu - \delta_{\mu\nu}Q^2\right)\Pi(Q^2)$$

Using analyticity

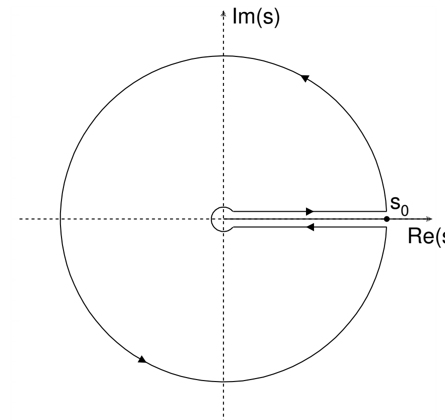

$$\Pi_{\mu\nu}(Q^2) = \frac{Q^2}{\pi}\int_{s_{\mathrm{th}}}^\infty \frac{\mathrm{Im}\Pi(s)}{s(s-Q^2-i\epsilon)}ds$$

Using unitarity (optical theorem)

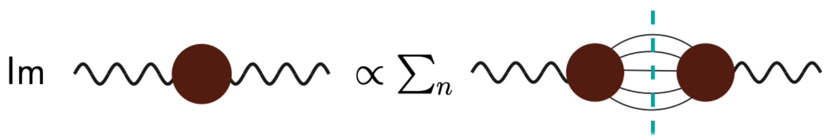

$$\mathrm{Im}\,\Pi(s) \propto \sigma(e^+e^- \to \gamma^* \to \mathrm{hadrons})$$

Finally, one gets the following dispersion relation (data-driven prediction):

Bouchiat and Michel, 1961

$$a_\mu^{\mathrm{HVP}} = \frac{\alpha^2}{3\pi^2}\int_{s_{\mathrm{th}}}^\infty ds\frac{K(s)}{s}R(s) \quad \text{with} \quad R(s) = \frac{\sigma(e^+e^- \to \mathrm{hadrons})}{\sigma(e^+e^- \to \mu^+\mu^-)}$$

Both cross sections at lowest order (bare cross sections)

Bare versus Dressed Cross Sections

It is important to emphasise that the cross sections in the R ratio, have to the bare one, namely corrected for initial state radiation (ISR), the effect of loops at the electron vertex and from leptonic and hadronic vacuum polarisation:

$$\sigma^{\text{bare}}(e^+e^- \to \text{hadrons}/\mu^+\mu^-) = \sigma^{\text{dressed}}(e^+e^- \to \text{hadrons}/\mu^+\mu^-)\left(\frac{\alpha(0)}{\alpha(s)}\right)^2$$

avoiding double counting in the higher order HVP contribution.

On the other hand, the final state radiation (FSR) has to be included in the (measured) bare cross sections.

Below 1 GeV, the corrections for the $\pi+\pi-$ cross sections are:

- ➢ −2.3% for leptonic vacuum polarisation
- ➢ Between −1.0 and +6.0% for hadronic vacuum polarisation
- ➢ +0.8% for FSR (all measurements expect BABAR rely on MC for the correction)

QED Kernel

Brodsky, de Rafael, 1968

The QED kernel has the following analytical form

$$K(s) = x^2\left(1-\frac{x^2}{2}\right)+(1+x)^2\left(1+\frac{1}{x^2}\right)\left(\ln(1+x)-x+\frac{x^2}{2}\right)+\frac{1+x}{1-x}x^2\ln x$$

with $x = \frac{1-\beta_\mu}{1+\beta_\mu}$ and $\beta_\mu = \sqrt{1-\frac{4m_\mu^2}{s}}$

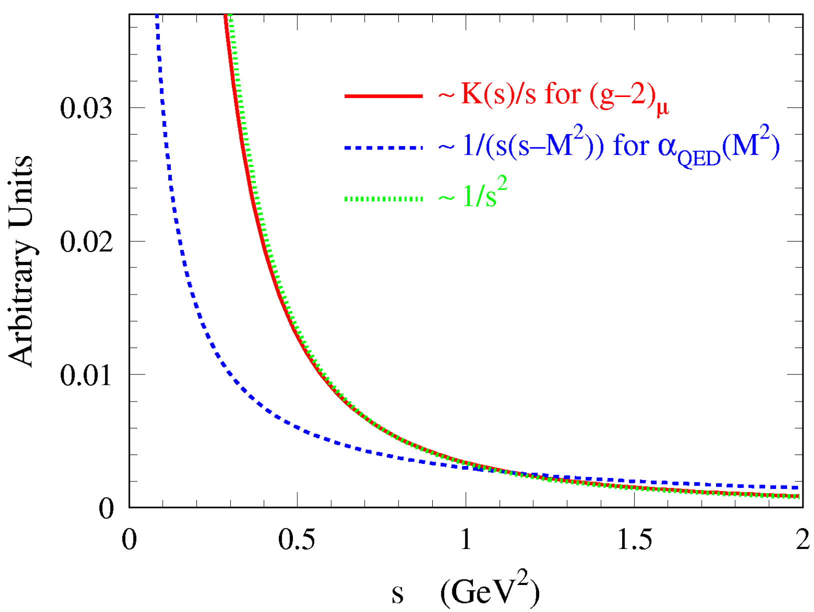

It has such an energy dependence that the cross section data at low energies are strongly weighted

Indeed, as we will see later that the $e^+e^-\to\pi^+\pi^-$ channel contributes 73% and about the same amount to the uncertainty

➔ The precision of the LO HVP prediction depends on that of the input data

R(s)

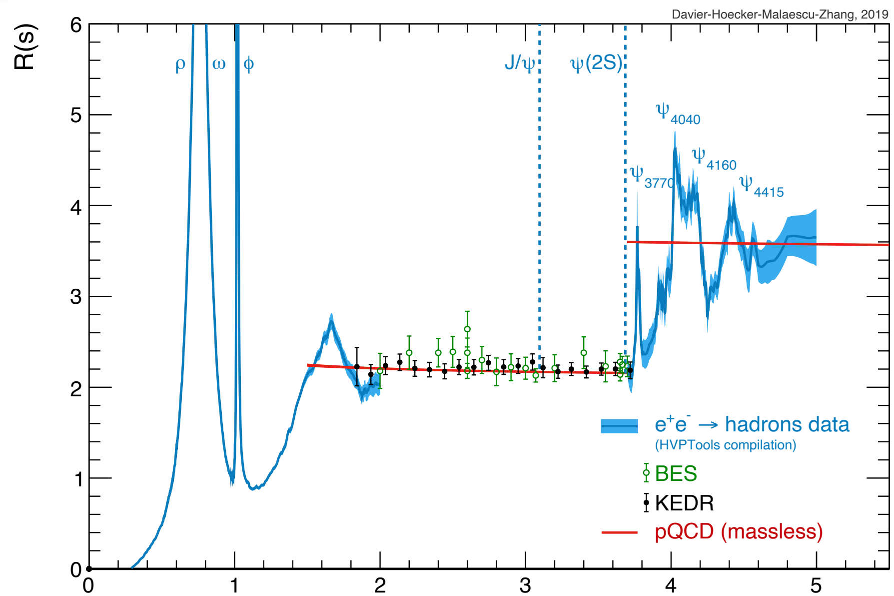

New BESIII measurements 2022 (14 data points between 2.2324 and 3.6710 GeV) with improved precision not shown

Quark parton model (QPM) prediction:

$$R(s)^{\text{QPM}} \simeq N_c \sum_q Q_q^2$$

≃ 10/3 for N_q=4

≃ 2 for N_q=3

Davier-Hoecker-Zhang, RMP 78 (2006) 1043

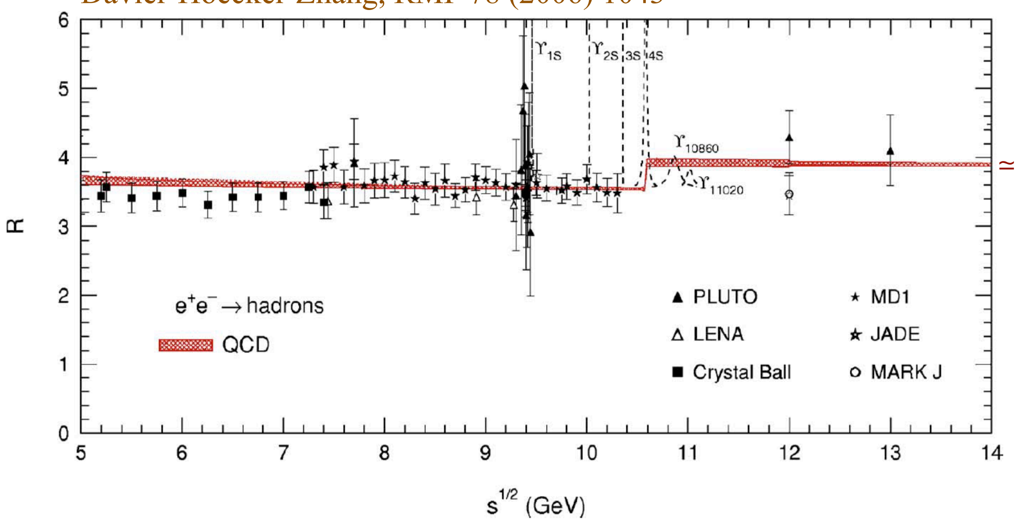

≃ 11/3 for N_q=5

- [$\pi^0\gamma$-1.8GeV]
  - sum about 22→37 exclusive channels
  - estimate unmeasured channels using isospin relations (now < 0.1%)
- [1.8-3.7] GeV
  - good agreement between data and pQCD calculation → use 4-loop pQCD
  - J/ψ, ψ(2s): Breit-Wigner integral
- [3.7-5] GeV
  use data
- >5GeV
  use 4-loop pQCD calculation

Contribution from exclusive channels at low energy

Channel	$a_\mu^{\rm HVP,LO}$ $[10^{-10}]$	$\Delta\alpha_{\rm had}(m_Z^2)$ $[10^{-4}]$
$\pi^0\gamma$	$4.29 \pm 0.06 \pm 0.04 \pm 0.07$	$0.35 \pm 0.00 \pm 0.00 \pm 0.01$
$\eta\gamma$	$0.65 \pm 0.02 \pm 0.01 \pm 0.01$	$0.08 \pm 0.00 \pm 0.00 \pm 0.00$
$\pi^+\pi^-$	$507.80 \pm 0.83 \pm 3.19 \pm 0.60$	$34.49 \pm 0.06 \pm 0.20 \pm 0.04$
$\pi^+\pi^-\pi^0$	$46.20 \pm 0.40 \pm 1.10 \pm 0.86$	$4.60 \pm 0.04 \pm 0.11 \pm 0.08$
$2\pi^+2\pi^-$	$13.68 \pm 0.03 \pm 0.27 \pm 0.14$	$3.58 \pm 0.01 \pm 0.07 \pm 0.03$
$\pi^+\pi^-2\pi^0$	$18.03 \pm 0.06 \pm 0.48 \pm 0.26$	$4.45 \pm 0.02 \pm 0.12 \pm 0.07$
$2\pi^+2\pi^-\pi^0$ (η excl.)	$0.69 \pm 0.04 \pm 0.06 \pm 0.03$	$0.21 \pm 0.01 \pm 0.02 \pm 0.01$
$\pi^+\pi^-3\pi^0$ (η excl.)	$0.49 \pm 0.03 \pm 0.09 \pm 0.00$	$0.15 \pm 0.01 \pm 0.03 \pm 0.00$
$3\pi^+3\pi^-$	$0.11 \pm 0.00 \pm 0.01 \pm 0.00$	$0.04 \pm 0.00 \pm 0.00 \pm 0.00$
$2\pi^+2\pi^-2\pi^0$ (η excl.)	$0.71 \pm 0.06 \pm 0.07 \pm 0.14$	$0.25 \pm 0.02 \pm 0.02 \pm 0.05$
$\pi^+\pi^-4\pi^0$ (η excl., isospin)	$0.08 \pm 0.01 \pm 0.08 \pm 0.00$	$0.03 \pm 0.00 \pm 0.03 \pm 0.00$
$\eta\pi^+\pi^-$	$1.19 \pm 0.02 \pm 0.04 \pm 0.02$	$0.35 \pm 0.01 \pm 0.01 \pm 0.01$
$\eta\omega$	$0.35 \pm 0.01 \pm 0.02 \pm 0.01$	$0.11 \pm 0.00 \pm 0.01 \pm 0.00$
$\eta\pi^+\pi^-\pi^0$(non$-\omega,\phi$)	$0.34 \pm 0.03 \pm 0.03 \pm 0.04$	$0.12 \pm 0.01 \pm 0.01 \pm 0.01$
$\eta 2\pi^+2\pi^-$	$0.02 \pm 0.01 \pm 0.00 \pm 0.00$	$0.01 \pm 0.00 \pm 0.00 \pm 0.00$
$\omega\eta\pi^0$	$0.06 \pm 0.01 \pm 0.01 \pm 0.00$	$0.02 \pm 0.00 \pm 0.00 \pm 0.00$
$\omega\pi^0$ ($\omega \to \pi^0\gamma$)	$0.94 \pm 0.01 \pm 0.03 \pm 0.00$	$0.20 \pm 0.00 \pm 0.01 \pm 0.00$
$\omega 2\pi$ ($\omega \to \pi^0\gamma$)	$0.07 \pm 0.00 \pm 0.00 \pm 0.00$	$0.02 \pm 0.00 \pm 0.00 \pm 0.00$
ω (non$-3\pi,\pi\gamma,\eta\gamma$)	$0.04 \pm 0.00 \pm 0.00 \pm 0.00$	$0.00 \pm 0.00 \pm 0.00 \pm 0.00$
K^+K^-	$23.08 \pm 0.20 \pm 0.33 \pm 0.21$	$3.35 \pm 0.03 \pm 0.05 \pm 0.03$
K_SK_L	$12.82 \pm 0.06 \pm 0.18 \pm 0.15$	$1.74 \pm 0.01 \pm 0.03 \pm 0.02$
ϕ (non$-K\overline{K},3\pi,\pi\gamma,\eta\gamma$)	$0.05 \pm 0.00 \pm 0.00 \pm 0.00$	$0.01 \pm 0.00 \pm 0.00 \pm 0.00$
$K\overline{K}\pi$	$2.45 \pm 0.05 \pm 0.10 \pm 0.06$	$0.78 \pm 0.02 \pm 0.03 \pm 0.02$
$K\overline{K}2\pi$	$0.85 \pm 0.02 \pm 0.05 \pm 0.01$	$0.30 \pm 0.01 \pm 0.02 \pm 0.00$
$K\overline{K}3\pi$ (estimate)	$-0.02 \pm 0.01 \pm 0.01 \pm 0.00$	$-0.01 \pm 0.00 \pm 0.00 \pm 0.00$
$\eta\phi$	$0.33 \pm 0.01 \pm 0.01 \pm 0.00$	$0.11 \pm 0.00 \pm 0.00 \pm 0.00$
$\eta K\overline{K}$ (non$-\phi$)	$0.01 \pm 0.01 \pm 0.01 \pm 0.00$	$0.00 \pm 0.00 \pm 0.01 \pm 0.00$
$\omega K\overline{K}$ ($\omega \to \pi^0\gamma$)	$0.01 \pm 0.00 \pm 0.00 \pm 0.00$	$0.00 \pm 0.00 \pm 0.00 \pm 0.00$
$\omega 3\pi$ ($\omega \to \pi^0\gamma$)	$0.06 \pm 0.01 \pm 0.01 \pm 0.01$	$0.02 \pm 0.00 \pm 0.00 \pm 0.00$
7π ($3\pi^+3\pi^-\pi^0$ + estimate)	$0.02 \pm 0.00 \pm 0.01 \pm 0.00$	$0.01 \pm 0.00 \pm 0.00 \pm 0.00$

➔ ~30 exclusive channels are integrated up to 1.8 GeV

The $\pi^+\pi^-$ channel is by far the dominant one

Relative contributions to a_μ from missing channels (estimated based on isospin symmetry)

→ 0.87 ± 0.15 % (DEHZ 2003)
→ 0.69 ± 0.07 % (DHMZ 2010)
→ 0.09 ± 0.02 % (DHMZ 2017)
→ 0.016 ± 0.016 % (DHMZ 2019)
(*Nearly complete set of exclusive measurements from BABAR*)

e^+e^- Machines and Experiments

Jegerlehner, 2012

Year	Accelerator	E_{max} (GeV)	Experiments	Laboratory
1961-1962	AdA	0.250		LNF Frascati (Italy)
1965-1973	ACO	0.6-1.1	DM1	Orsay (France)
1967-1970	VEPP-2	1.02-1.4	'spark chamber'	Novosibirsk (Russia)
1967-1993	ADONE	3.0	BCF,$\gamma\gamma$, $\gamma\gamma$2, MEA, $\mu\pi$, FENICE	LNF Frascati (Italy)
1971-1973	CEA	4,5		Cambridge (USA)
1972-1990	SPEAR	2.4-8	MARK I, CB, MARK 2	SLAC Stanford (USA)
1974-1992	DORIS	-11	ARGUS, CB, DASP 2, LENA, PLUTO	DESY Hamburg (D)
1975-1984	DCI	3.7	DM1,DM2,M3N,B$\bar{\text{B}}$	Orsay (France)
1975-2000	VEPP-2M	0.4-1.4	OLYA, CMD, CMD-2, ND,SND	Novosibirsk (Russia)
1978-1986	PETRA	12-47	PLUTO, CELLO, JADE, MARK-J, TASSO	DESY Hamburg (D)
1979-1985	VEPP-4	-11	MD1	Novosibirsk (Russia)
1979-2008	CESR/CESR-C	9-12	CLEO, CUSB	Cornell (USA)
1980-1990	PEP	-29	MAC, MARK-2	SLAC Stanford (USA)
1987-1995	TRISTAN	50-64	AMY, TOPAZ, VENUS	KEK Tsukuba (Japan)
1989	SLC	90 GeV	SLD	SLAC Stanford (USA)
1989-2005	BEPC	2.0-4.8	BES, BES-II	IHEP Beijing (China)
1989-2000	LEP I/II	110/210	ALEPH, DELPHI, L3, OPAL	CERN Geneva (CH)
1994-	VEPP-4M	12	KEDR	Novosibirsk (Russia)
1999-2007	DAΦNE	Φ factory	KLOE	LNF Frascati (Italy)
1999-2008	PEP-II	*B* factory	BaBar	SLAC Stanford (USA)
1999-2010	KEKB	*B* factory	Belle	KEK Tsukuba (Japan)
2008-	BEPC-II		BES-III	IHEP Beijing (China)
2010-	VEPP-2000	2	SND, CMD-3	Novosibirsk (Russia)
2015-	SuperKEKB	*B* factory		KEK Tsukuba (Japan)

Long history

- Exclusive channels at low energy (below ~1.8 GeV) and

- Inclusive one at higher energy (above ~2 GeV)

measured by many experiments at low energy machines

Early versus Recent Measurements

Early measurements (DM1, DM2, OLYA, CMD, …)

- ☹️ Limited detector performance
- ☹️ Low luminosity
- ☹️ Unspecified radiative corrections

Recent measurements (CMD-2/3, SND, BES (II/III), BABAR, KLOE, …)

- 🙂 Better detectors
- 🙂 High luminosity machines
- 🙂 Bare cross section

Energy Scan versus ISR Method

1. The scan method: e.g. CMD-2/3, SND at Novosibirsk
   - ➢ Advantages:
     - ➢ Well defined $\sqrt{s}$
     - ➢ Good energy resolution $\sim 10^{-3}\sqrt{s}$
     - ➢ Background is small
   - ➢ Disadvantages:
     - ➢ Energy gap between two scans
     - ➢ Low luminosity at low energies
     - ➢ Limited $\sqrt{s}$ range of a given experiment
     - ➢ Normalisation is energy point dependent

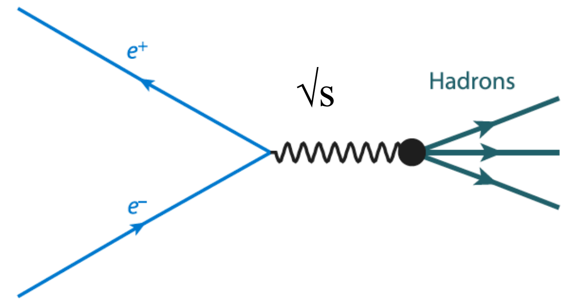

2. The ISR approach: e.g. BABAR, KLOE, BES
   - ➢ Advantages:
     - ➢ $\sigma(e^+e^- \to \text{hadrons})$ may be measured over $\sigma(e^+e^- \to \mu^+\mu^-)$ thus reducing some syst uncertainties
     - ➢ Continuous cross section measurement over a broad energy range down to threshold
   - ➢ Disadvantages:
     - ➢ Need to control background processes
     - ➢ Limited energy resolution from visible final state
     - ➢ Higher order process but compensated by higher luminosity of colliders running at a meson resonance

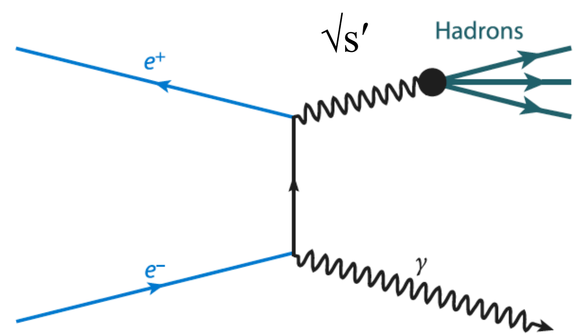

$s' = (1-x)/s$

$x = 2E_\gamma/\sqrt{s}$

ISR versus FSR Photons

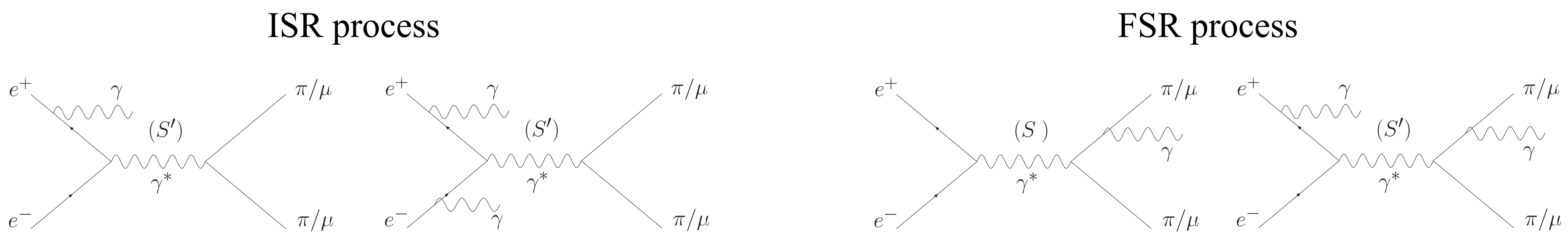

Theoretically the FSR contribution is not negligible though suppressed
- wrt to small angle ISR photons in the KLOE analyses
- due to higher $\sqrt{s}$ for BABAR as $|FSR|^2 \propto |F_\pi(s)|^2$

Experimentally one cannot separate FSR from large angle (LA) ISR on an event-by-event basis but one has a good statistical separation at BABAR

DHLMZ23

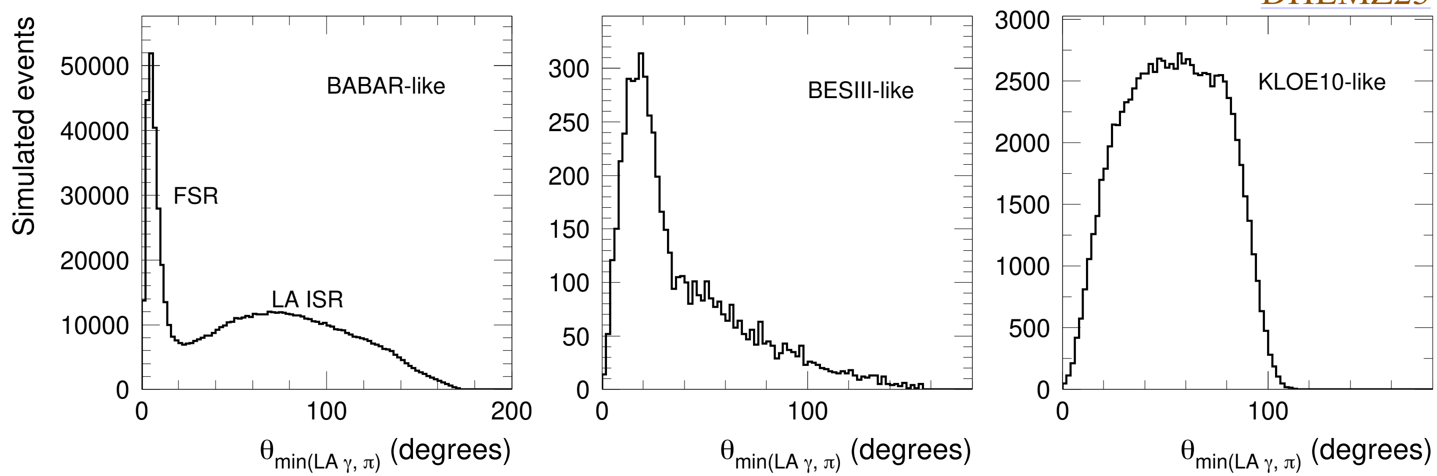

Tagged versus Untagged ISR Photon

Tagged ISR analysis at large angles within the detector acceptance (e.g. BABAR, KLOE10)

- 🙂 Background is small
- 🙂 Hard ISR photons (softer for KLOE since $\sqrt{s}$ = 1.02 GeV (KLOE) vs 10.58 GeV for BABAR)
- 🙂 Since the full event is observed, BABAR performs kinematic fits to incorporate undetected additional ISR or detected FSR photon

Untagged ISR analysis at small angles (e.g. KLOE08, KLOE12)

- 🙂 Background suppressed by requiring that the missing momentum of the event is collinear with the beam axis
- 🙁 Larger background from two-photon processes
- 🙁 Small-angle ISR photons (out of the detector acceptance) undetected

Additional difference between (KLOE08 and KLOE10) and (BABAR and KLOE12)
- the former relies on the NLO Phokhara MC to determine the ISR luminosity
- the latter is derived from $\pi\pi(\gamma)/\mu\mu(\gamma)$ ratio where some of the uncertainties cannel

Measurements of 2π Channel: CMD-2, SND

CMD-2 (2006)
- Energy 0.35-0.52 GeV

JETP Lett. 84, 413 (2006) (link)

- Energy 0.6-1.0 GeV

Phys. Lett. B 648, 28 (2007) (link)

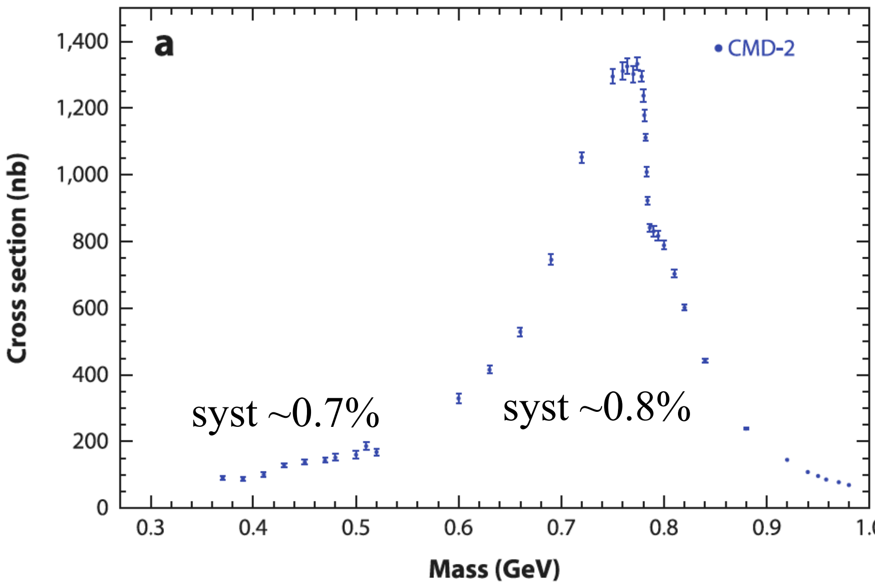

Figures a, b from M. Davier, Ann. Rev. Nucl. Part. Sci. 63 (2013) 407 (link)

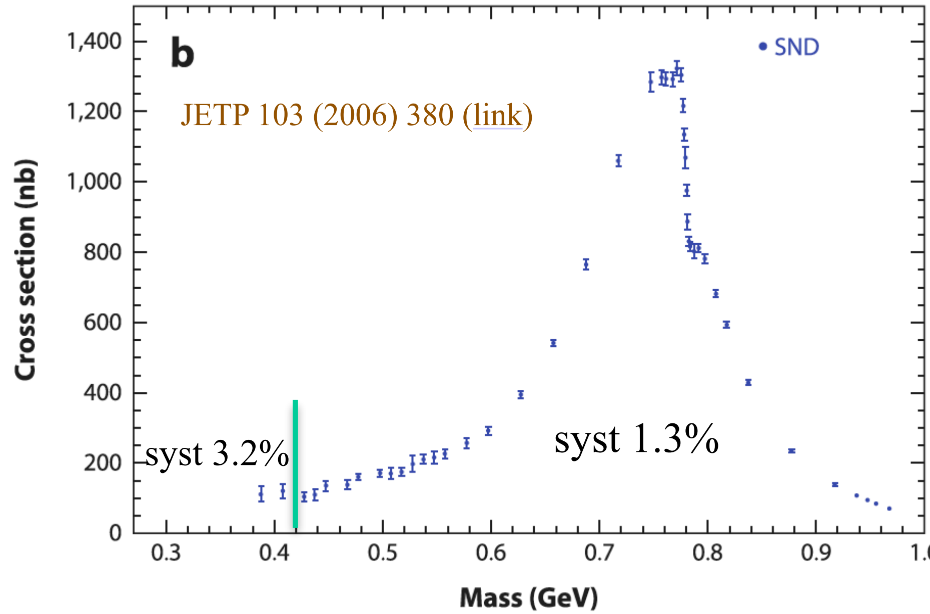

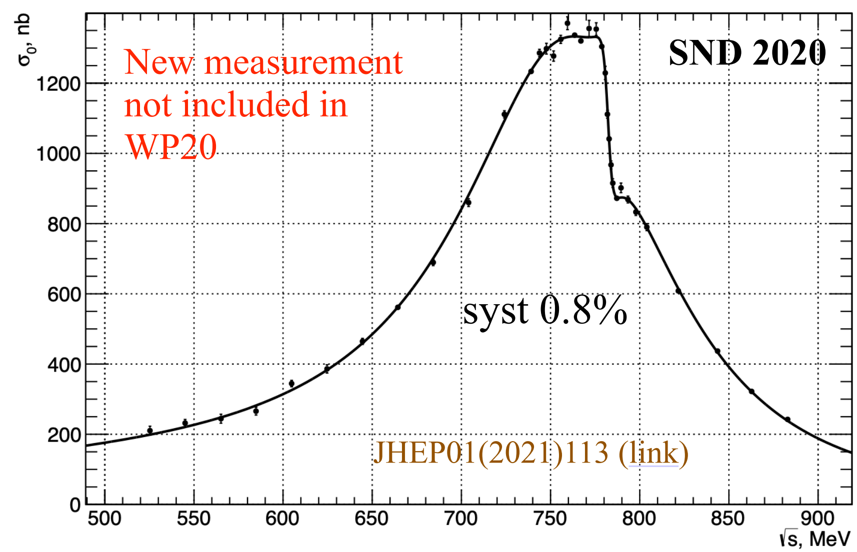

Measurements of 2π Channel: KLOE 08,10,12

$\sqrt{s}$=1.02 GeV ⇒ Soft ISR photons

Figure 3 from WP20

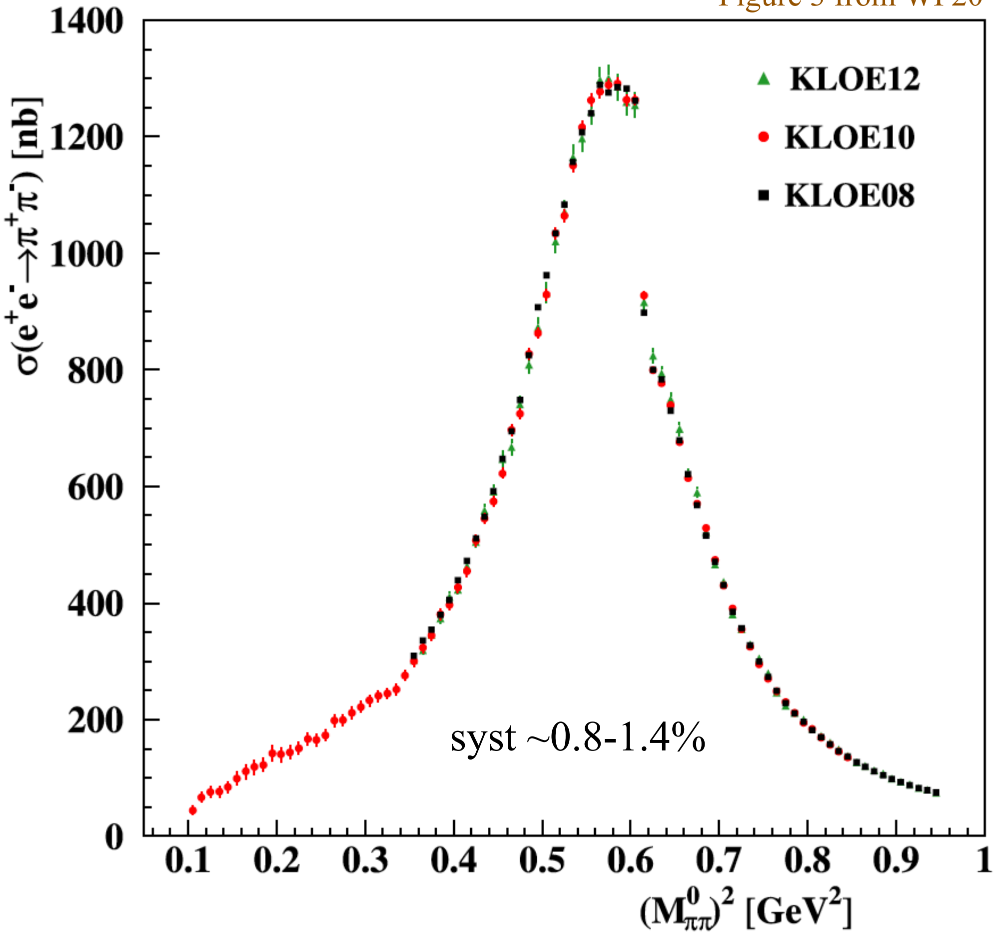

- KLOE12: photon at small angle and undetected, radiator function from measured $\mu^+\mu^-(\gamma)$ events
- KLOE10: photon at large angle and detected, radiator function from NLO QED
- KLOE08: photon at small angle and undetected, radiator function from NLO QED

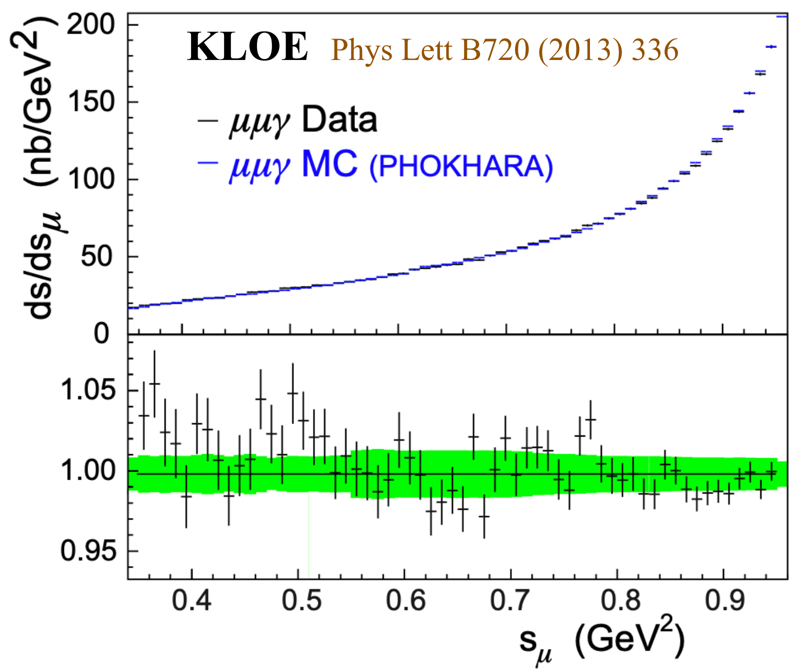

Quoted Uncertainties and Correlations (KLOE)

	$\sigma_{\pi\pi\gamma}$	$\sigma^0_{\pi\pi}$	F_π	$\Delta^{\pi\pi}a_\mu$
Reconstruction Filter	negligible			
Background subtraction	Tab. 1			0.3%
Trackmass	0.2%			
Pion cluster ID	negligible			
Tracking efficiency	0.3%			
Trigger efficiency	0.1%			
Acceptance	Tab. 2			0.2%
Unfolding	Tab. 3			negligible
L3 filter	0.1%			
$\sqrt{s}$ dependence of H	-	Tab. 4		0.2%
Luminosity	0.3%			
Experimental systematics				0.6%
FSR resummation	-	0.3%		
Radiator function H	-	0.5%		
Vacuum Polarization	-	0.1%	-	0.1%
Theory systematics				0.6%

$M^2_{\pi\pi}$ range (GeV^2)	Systematic error (%)
$0.35 \leq M^2_{\pi\pi} < 0.39$	0.6
$0.39 \leq M^2_{\pi\pi} < 0.43$	0.5
$0.43 \leq M^2_{\pi\pi} < 0.45$	0.4
$0.45 \leq M^2_{\pi\pi} < 0.49$	0.3
$0.49 \leq M^2_{\pi\pi} < 0.51$	0.2
$0.51 \leq M^2_{\pi\pi} < 0.64$	0.1
$0.64 \leq M^2_{\pi\pi} < 0.95$	-

KLOE 08 (arXiv:0809.3950)

KLOE 10 (arXiv:1006.5313)

	$\sigma_{\pi\pi\gamma}$	$\sigma^{\text{bare}}_{\pi\pi}$	$\|F_\pi\|^2$	$\Delta a^{\pi\pi}_\mu$ (0.1 - 0.85 GeV^2)
	threshold ; ρ-peak			
Background Filter	0.5% ; 0.1%			negligible
Background subtraction	3.4% ; 0.1%			0.5%
$f_0 + \rho\pi$ bkg.	6.5% ; negl.			0.4%
Ω cut	1.4% ; negl.			0.2%
Trackmass cut	3.0% ; 0.2%			0.5%
π-e PID	0.3% ; negl.			negligible
Trigger	0.3% ; 0.2%			0.2%
Acceptance	1.9% ; 0.3%			0.5%
Unfolding	negl. ; 2.0%			negligible
Tracking	0.3%			
Software Trigger (L3)	0.1%			
Luminosity	0.3%			
Experimental syst.				1.0%
FSR treatment	-	7% ; negl.		0.8%
Radiator function H	-	0.5%		
Vacuum Polarization	-	Ref. [34]	-	0.1%
Theory syst.				0.9%

Systematics *evaluated* in ~wide mass ranges with sharp transitions

Measurements of 2π Channel: BABAR 09

$\sqrt{s}$=10.58 GeV ⇒ Hard ISR photons

Figure 3 from WP20

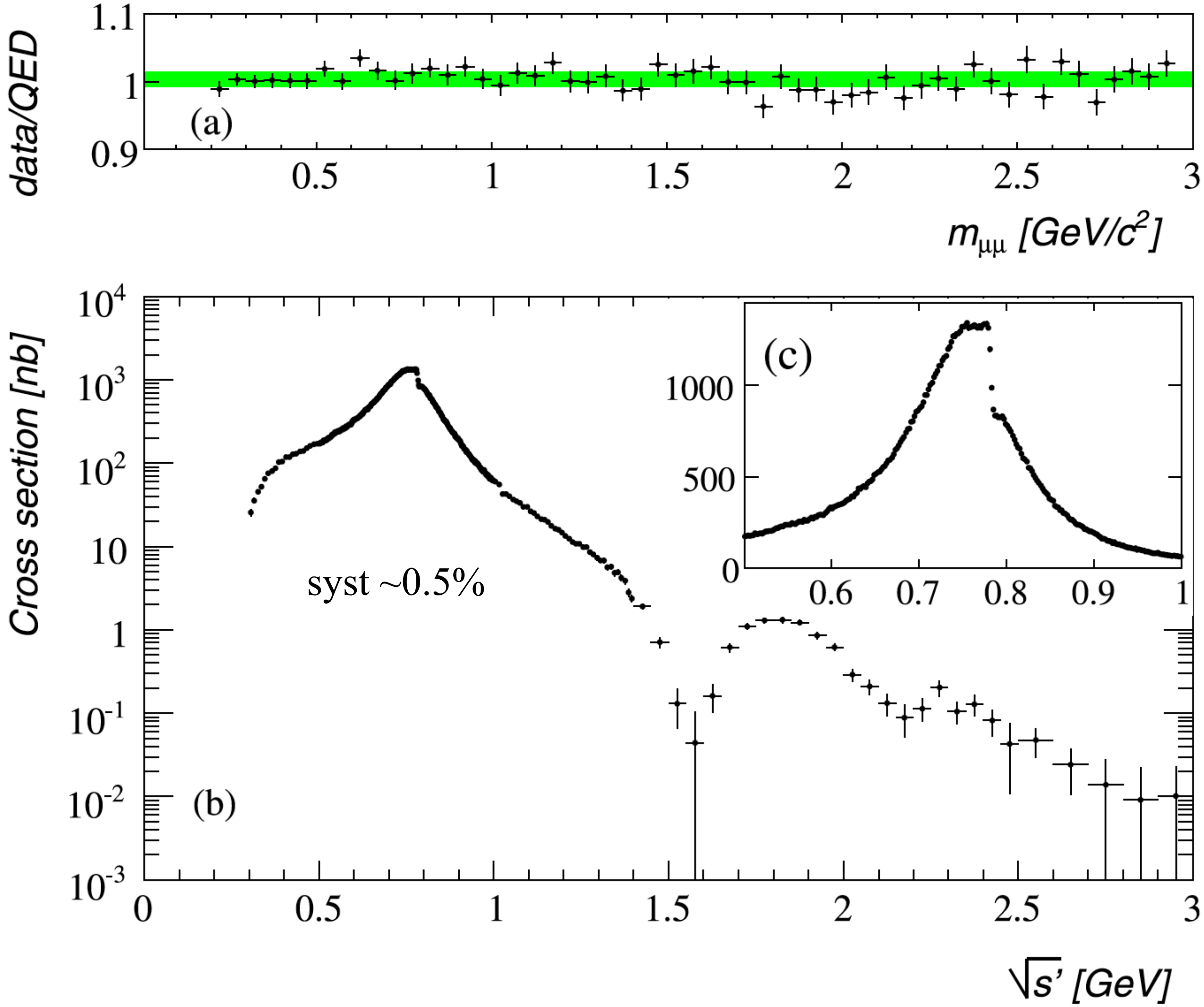

BABAR measurement covers a huge mass range from threshold to 3 GeV!

In BABAR, the ISR photon is detected at large angle

Both pion and muon pairs are measured and the ratio $\pi\pi(\gamma)/\mu\mu(\gamma)$ directly provides the $\pi\pi(\gamma)$ cross section

Quoted Uncertainties (BABAR)

BABAR (arXiv:1205.2228)

Sources	0.3-0.4	0.4-0.5	0.5-0.6	0.6-0.9	0.9-1.2	1.2-1.4	1.4-2.0	2.0-3.0
trigger/ filter	5.3	2.7	1.9	1.0	0.7	0.6	0.4	0.4
tracking	3.8	2.1	2.1	1.1	1.7	3.1	3.1	3.1
π-ID	10.1	2.5	6.2	2.4	4.2	10.1	10.1	10.1
background	3.5	4.3	5.2	1.0	3.0	7.0	12.0	50.0
acceptance	1.6	1.6	1.0	1.0	1.6	1.6	1.6	1.6
kinematic fit (χ^2)	0.9	0.9	0.3	0.3	0.9	0.9	0.9	0.9
correl $\mu\mu$ ID loss	3.0	2.0	3.0	1.3	2.0	3.0	10.0	10.0
$\pi\pi/\mu\mu$ non-cancel.	2.7	1.4	1.6	1.1	1.3	2.7	5.1	5.1
unfolding	1.0	2.7	2.7	1.0	1.3	1.0	1.0	1.0
ISR luminosity	3.4	3.4	3.4	3.4	3.4	3.4	3.4	3.4
sum (cross section)	13.8	8.1	10.2	5.0	6.5	13.9	19.8	52.4

All quoted uncertainties in 10^{-3}

Systematics *evaluated* in ~wide mass ranges with sharp transitions (statistics limitations when going to narrow ranges)

Measurements of 2π Channel: BESIII, CLEO-c

Original publication: Phys. Lett. B 753, 629 (2016)
Erratum: Phys. Lett. B 812, 135982 (2021) for updating the stat covariance matrix

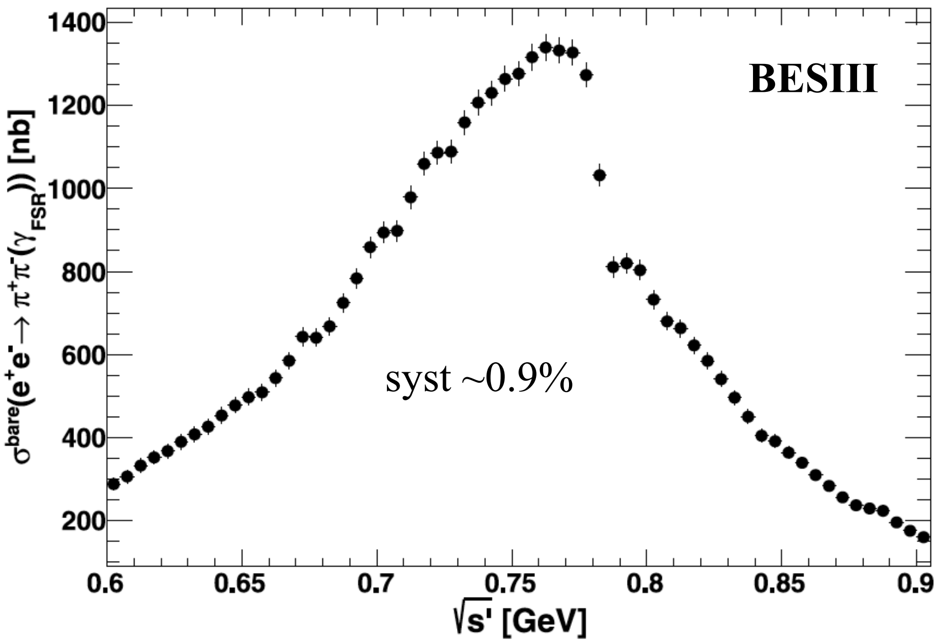

Phys. Rev. D 97, 032012 (2018)

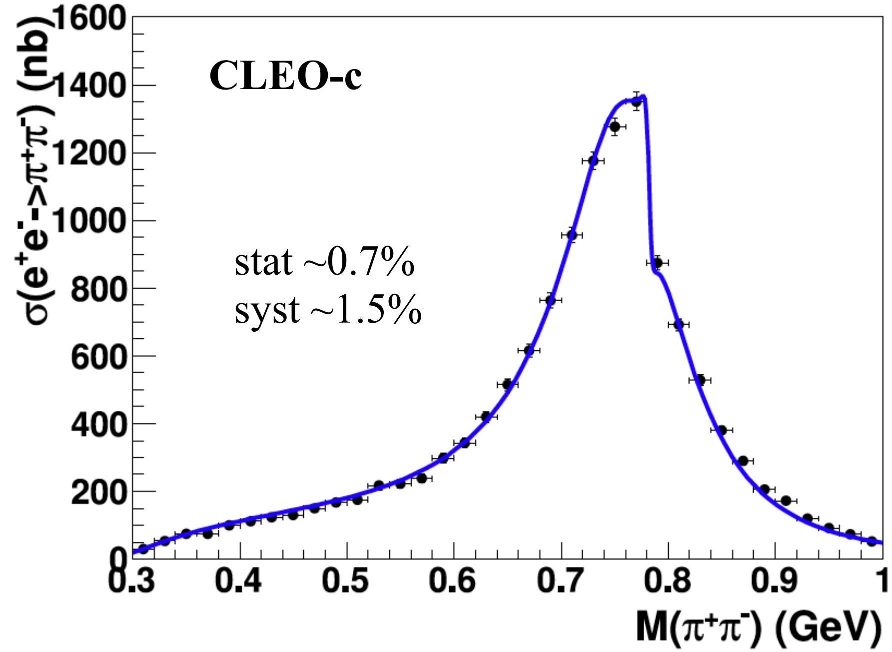

New Measurement of 2π Channel: CMD-3

Figures from CMD-3 (PRL)

Uncertainty ~0.7% achieved at the rho peak

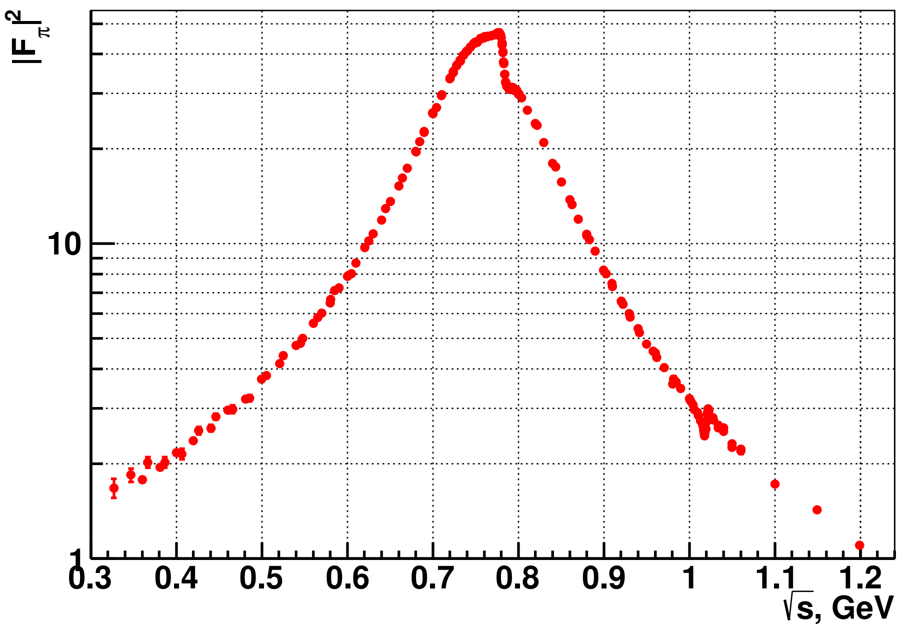

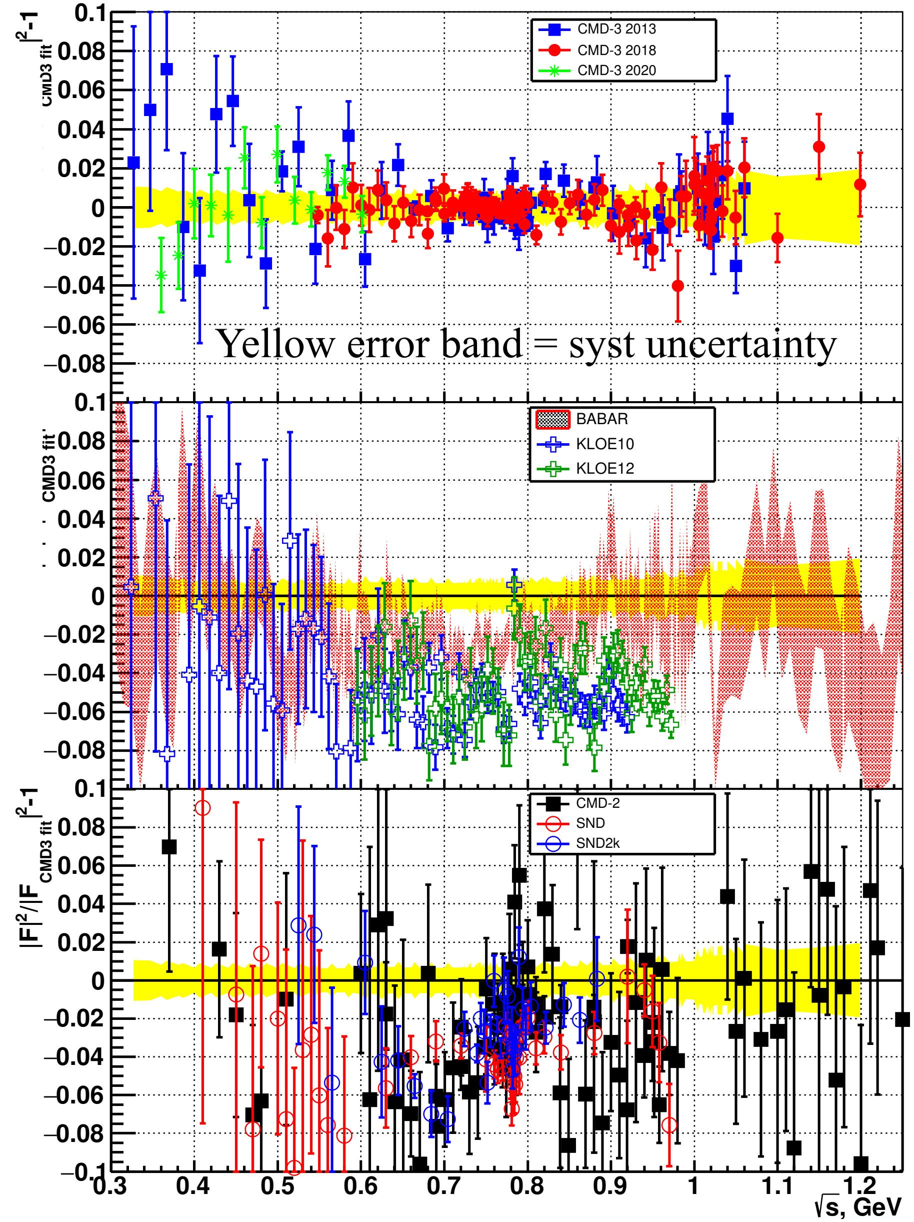

CMD-3 has improved detector, larger samples

Two panel Theory Initiatives (TI) discussions with 49 questions addressed to CMD-3 did not allow to identify any major problem

CMD-2 / CMD-3 tension still an open question

Comparison

Figure from DHMZ, EPJC80 (2020) 241

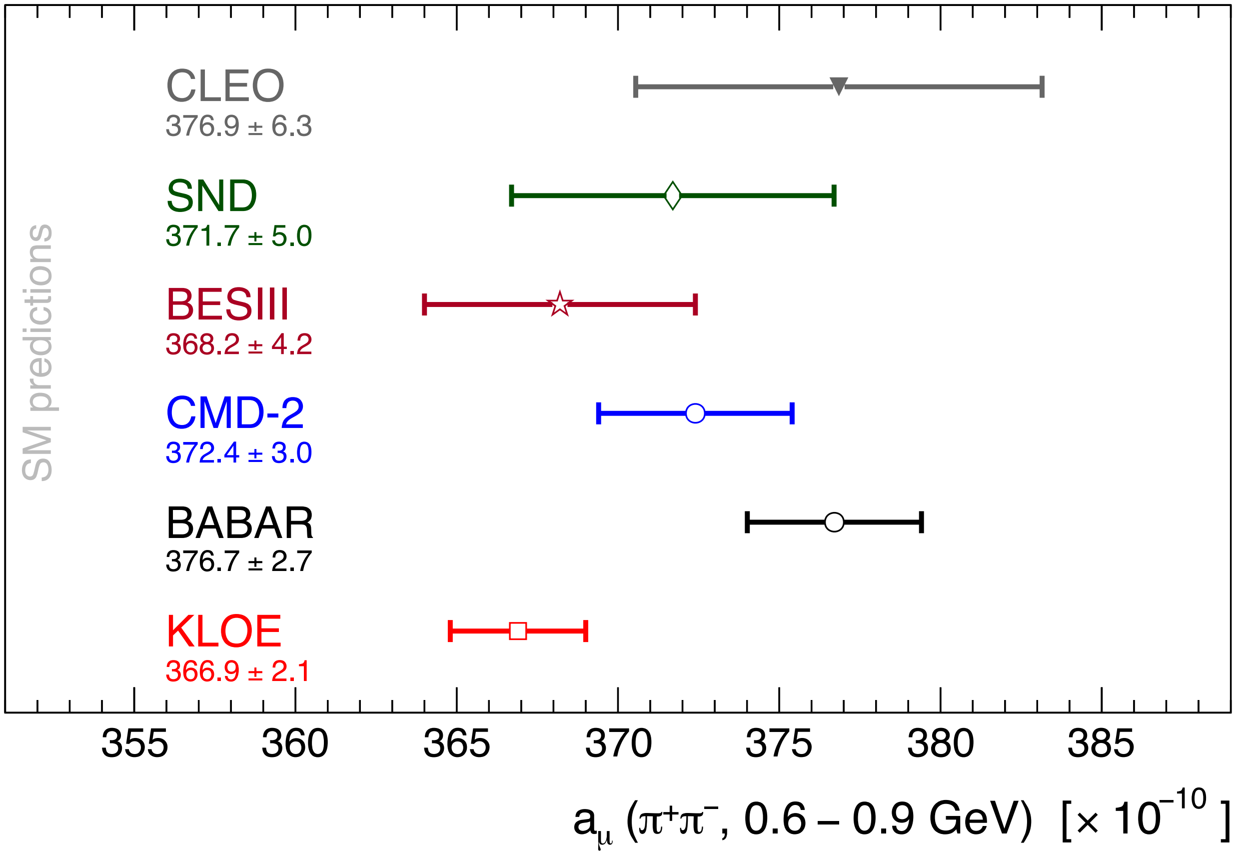

BABAR and KLOE most precise but in clear discrepancy
Combination needs special treatment (see later)

Data Combination Considerations

Goal: combine experimental spectra with arbitrary point spacing / binning

Requirements:

- Properly propagate uncertainties and correlations
  - *Between measurements (data points/bins) of a given experiment*
    (covariance matrices and/or detailed split of uncertainties in sub-components)
  - *Between experiments* (common systematic uncertainties, e.g. VP)
    based on detailed information provided in publications
  - *Between different channels* – identify common systematic uncertainties
    - BABAR luminosity (ISR or BhaBha), efficiencies (photon, K_S, K_L, modeling)
    - BABAR radiative corrections; $4\pi 2\pi^0 - \eta\omega$
    - CMD-2 $\eta\gamma - \pi^0\gamma$; CMD2/3 luminosity; SND luminosity
    - FSR; hadronic VP (old experiments)

(1st motivation for using DHMZ uncertainties as "baseline" in the g-2 TI White Paper)

- Minimise biases
- Optimise g-2 integral uncertainty

(*without overestimating the precision with which the uncertainties of the measurements are known*)

Combination Procedure Implemented in HVPTools

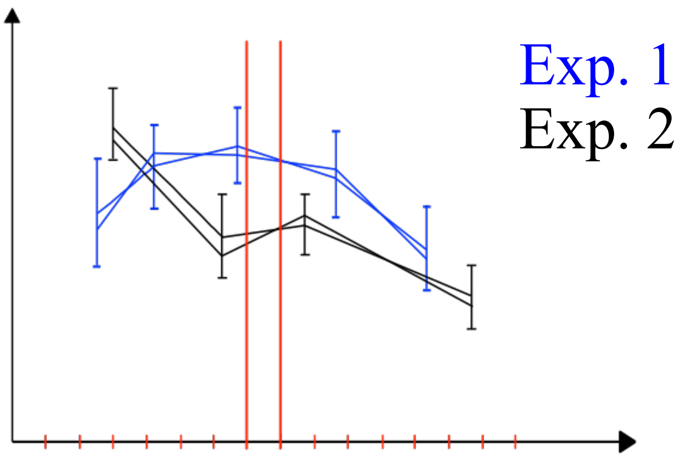

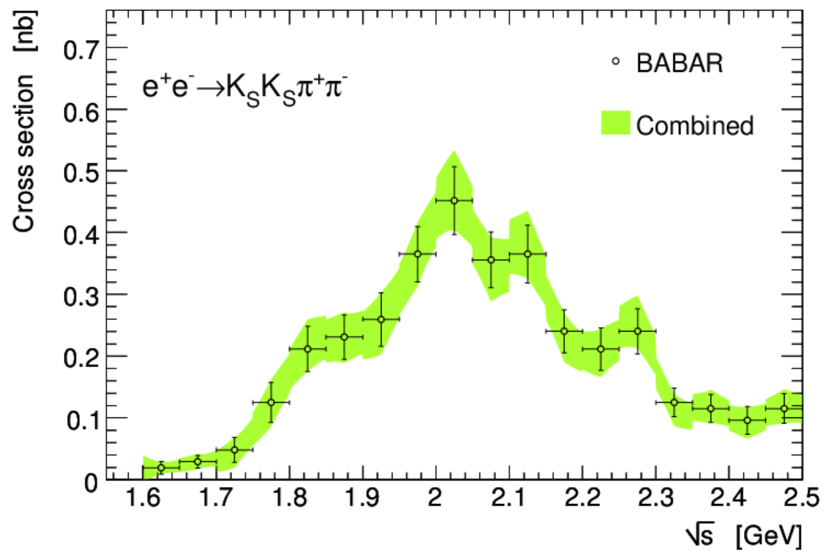

- Define a (fine) final binning (to be filled and used for integrals etc.)
- Linear/quadratic splines to interpolate between the points/bins of each experiment
  - for binned measurements: preserve integral inside each bin
  - closure test: replace nominal values of data points by Gounaris-Sakurai model and re-do the combination
  - ➔ *(non-)negligible bias for (linear)quadratic interpolation*
- Fluctuate data points taking into account correlations & re-do the splines for each (pseudo-)experiment
  - each uncertainty fluctuated coherently for all the points/bins that it impacts
  - eigenvector decomposition for (statistical) covariance matrices

Combination Procedure Implemented in HVPTools

For each final bin:

- Compute an average value for each measurement and its uncertainty
- Compute correlation matrix between experiments
- Minimise χ^2 and get average coefficients (weights)
- Compute average between experiments and its uncertainty

Evaluation of integrals and propagation of uncertainties:

- Integral(s) evaluated for nominal result and for each set of toy pseudo-experiments;
  uncertainty of integrals from RMS of results for all toys
- The pseudo-experiments also used to derive (statistical & systematic) covariance matrices
  of combined cross sections → Integral evaluation
- Uncertainties also propagated through $\pm1\sigma$ shifts of each uncertainty:
  allows to account for correlations between different channels (for integrals and spectra)
- Checked consistency between the different approaches

Combination Procedure: Weights of Various Experiments

For each final bin:

➢ Minimise χ^2 and get average coefficients

Note: average weights must account for bin sizes / point spacing of measurements (do not over-estimate the weight of experiments with large bins)

➢ Weights in fine bins evaluated using a common (large) binning for measurements + interpolation

➢ Compare the precisions on the same footing

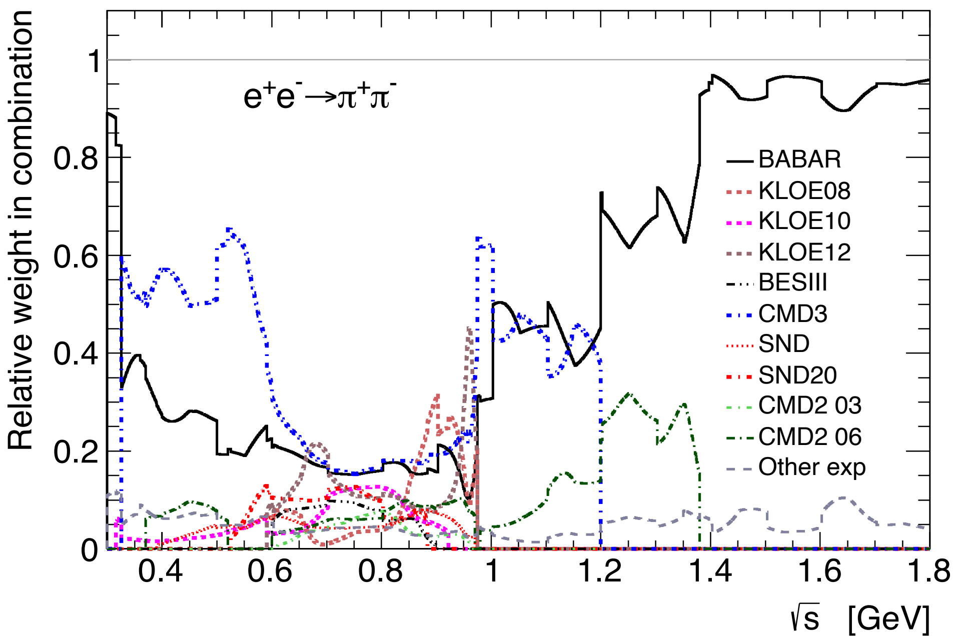

➢ Bins used by KLOE larger than the ones by BABAR in ρ-ω interference region (factor ~3)

➢ Average dominated by BABAR, CMD-3, KLOE, SND20

➢ BABAR covering full range

Combination Procedure: Compatibility between Measurements

For each final bin:

- χ^2 /ndof: test locally the level of agreement between input measurements, *taking into account correlations*
- Scale uncertainties in bins with χ^2 /ndof > 1 (PDG): *locally* conservative; Adopted by KNT since '17

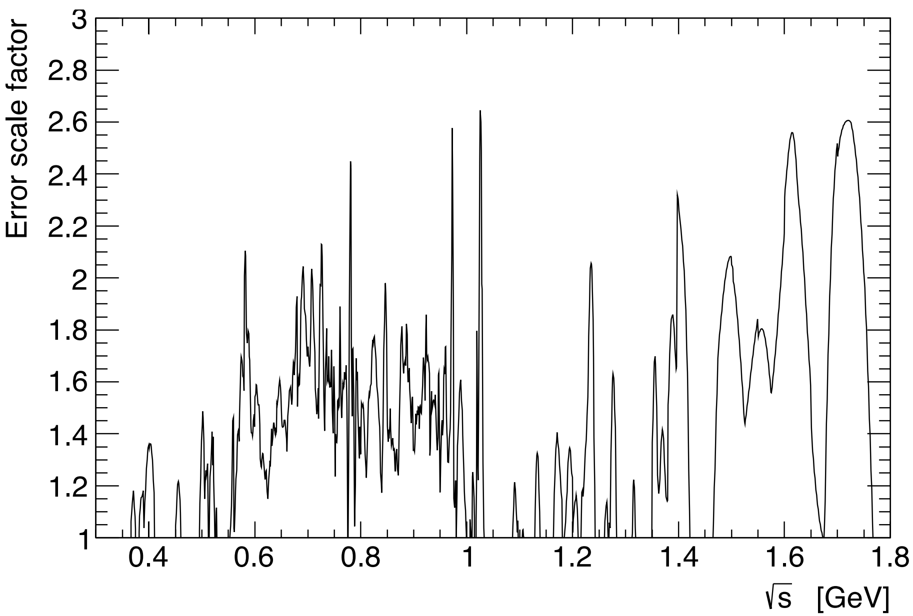

- Tension between measurements, especially between KLOE & CMD-3, which provide the smallest / largest cross-sections in the ρ region: Indication of underestimated uncertainties
  Motivates conservative uncertainty treatment in combination fit (evaluation of weights / fits based on analyticity & unitarity to constrain uncertainties at low √s)
- Observed (systematic) tension between measurements, beyond the local χ^2 /ndof rescaling

- (*Since 2019*) Included extra (dominant) uncertainty: 1/2 difference between integrals w/o either BABAR or KLOE *(2nd motivation for using DHMZ uncertainties as "baseline" in the TI WP)*
  Extra uncertainty started to be adopted in other studies (arXiv:2205.12963)
  However, tensions are larger now and we need to understand their source!

Combined 2π vs Individual Measurements (DHMZ19)

Figures from DHMZ, EPJC80 (2020) 241

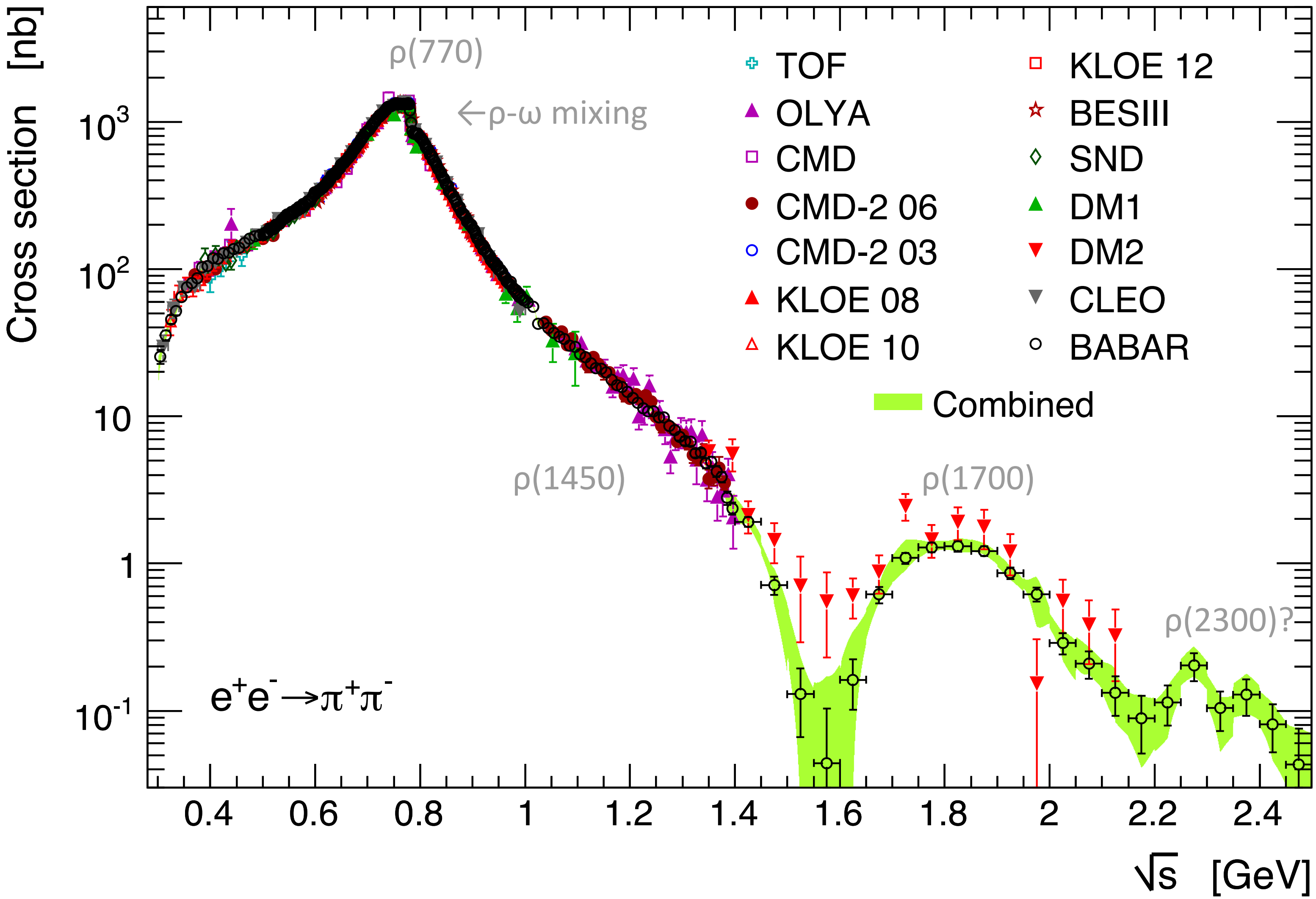

Combined 2π vs Individual Measurements (DHMZ19)

Figures from DHMZ, EPJC80 (2020) 241

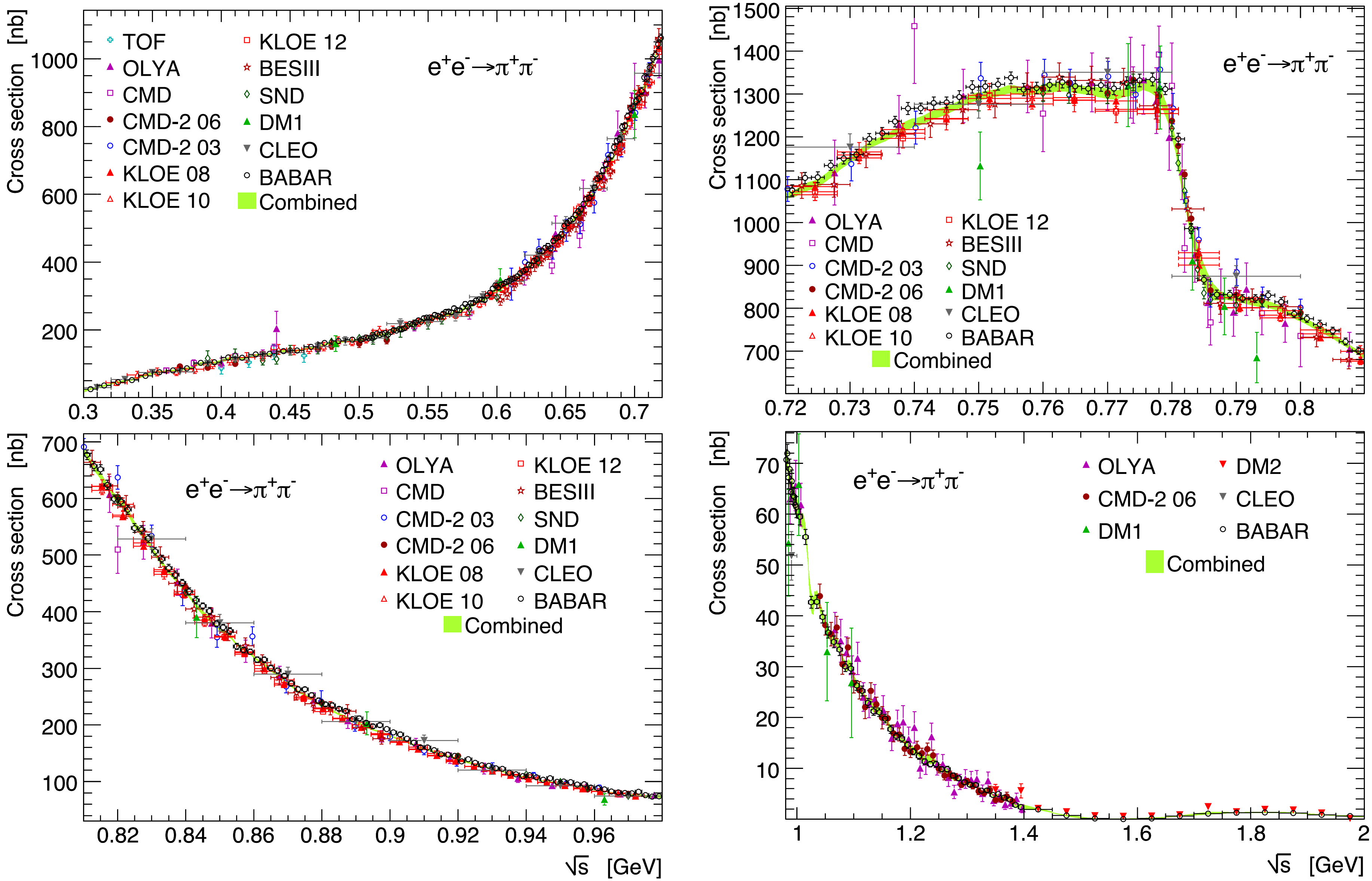

New Combination Including CMD-3, SND20, Updated BESIII

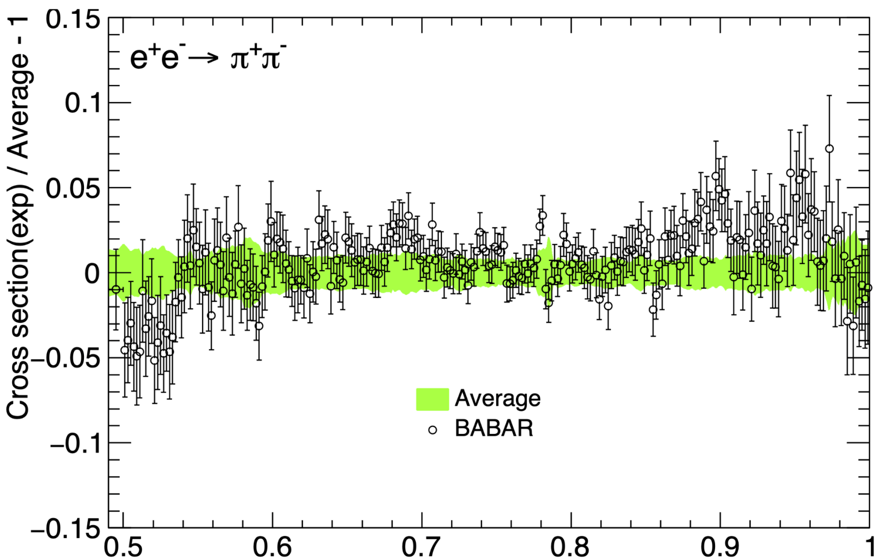

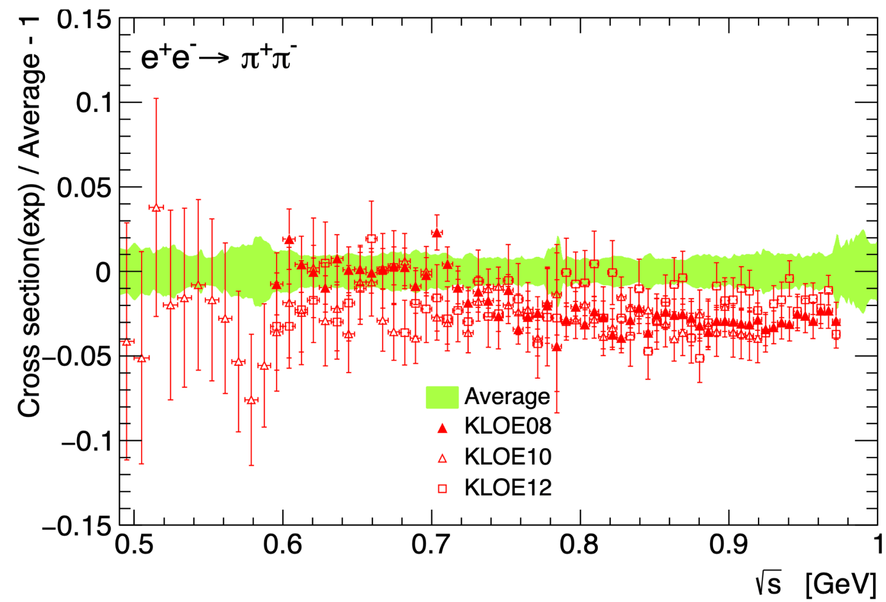

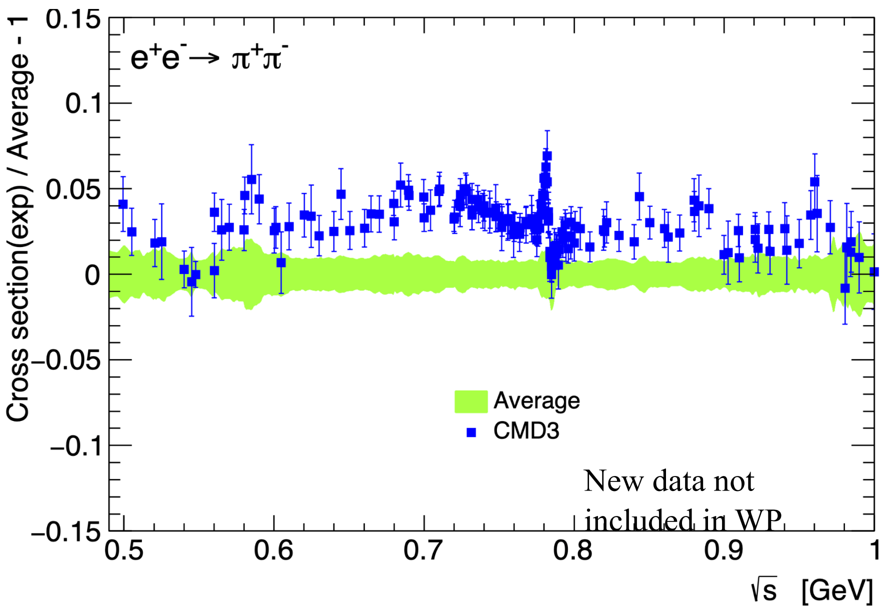

- The discrepancy among the three most precise measurements BABAR, CMD-3 and KLOE:
  - Over 5σ CMD-3 vs KLOE around ρ
  - Below 3σ BABAR vs CMD-3
- The discrepancy prevents improved precision of LO HVP predictions

Fit at Low Energy Based on Analyticity and Unitarity

Motivated by fewer measurements and poor precision at low energy, a fit was performed

Pion form factor F_π^0 extracted from $\pi^+\pi^-$ bare cross sections as in [1810.00007]

$$|F_\pi^0|^2 = |G(s) \times J(s)|^2$$

$$G(s) = 1 + \alpha_V s + \frac{\kappa s}{m_\omega^2 - s - i m_\omega \Gamma_\omega}$$

$$J(s) = e^{1-\frac{\delta_1(s_0)}{\pi}} \left(1 - \frac{s}{s_0}\right)^{\left[1-\frac{\delta_1(s_0)}{\pi}\right]\frac{s_0}{s}} \left(1 - \frac{s}{s_0}\right)^{-1} e^{\frac{s}{\pi}\int_{4m_\pi^2}^{s_0} dt \frac{\delta_1(t)}{t(t-s)}}$$

$$\cot \delta_1(s) = \frac{\sqrt{s}}{2k^3}\left(m_\rho^2 - s\right)\left[\frac{2m_\pi^3}{m_\rho^2\sqrt{s}} + B_0 + B_1\omega(s)\right]$$

$$k = \frac{\sqrt{s - 4m_\pi^2}}{2}$$

$$\omega(s) = \frac{\sqrt{s} - \sqrt{s_0 - s}}{\sqrt{s} + \sqrt{s_0 - s}}$$

$$\sqrt{s_0} = 1.05 \text{ GeV}$$

$G(s)$ from [arXiv:1611.09359]
$J(s)$ from [hep-ph/0106025, 0402285]
$\cot\delta_1(s)$ from [arXiv:1102.2183]

Six free parameters to fit:
α_V, κ, m_ω, m_ρ, B_0, B_1
(Γ_ω fixed to PDG value)

Fit Performed to 1 GeV, Results Used to 0.6 GeV

Figures from DHMZ, EPJC80 (2020) 241

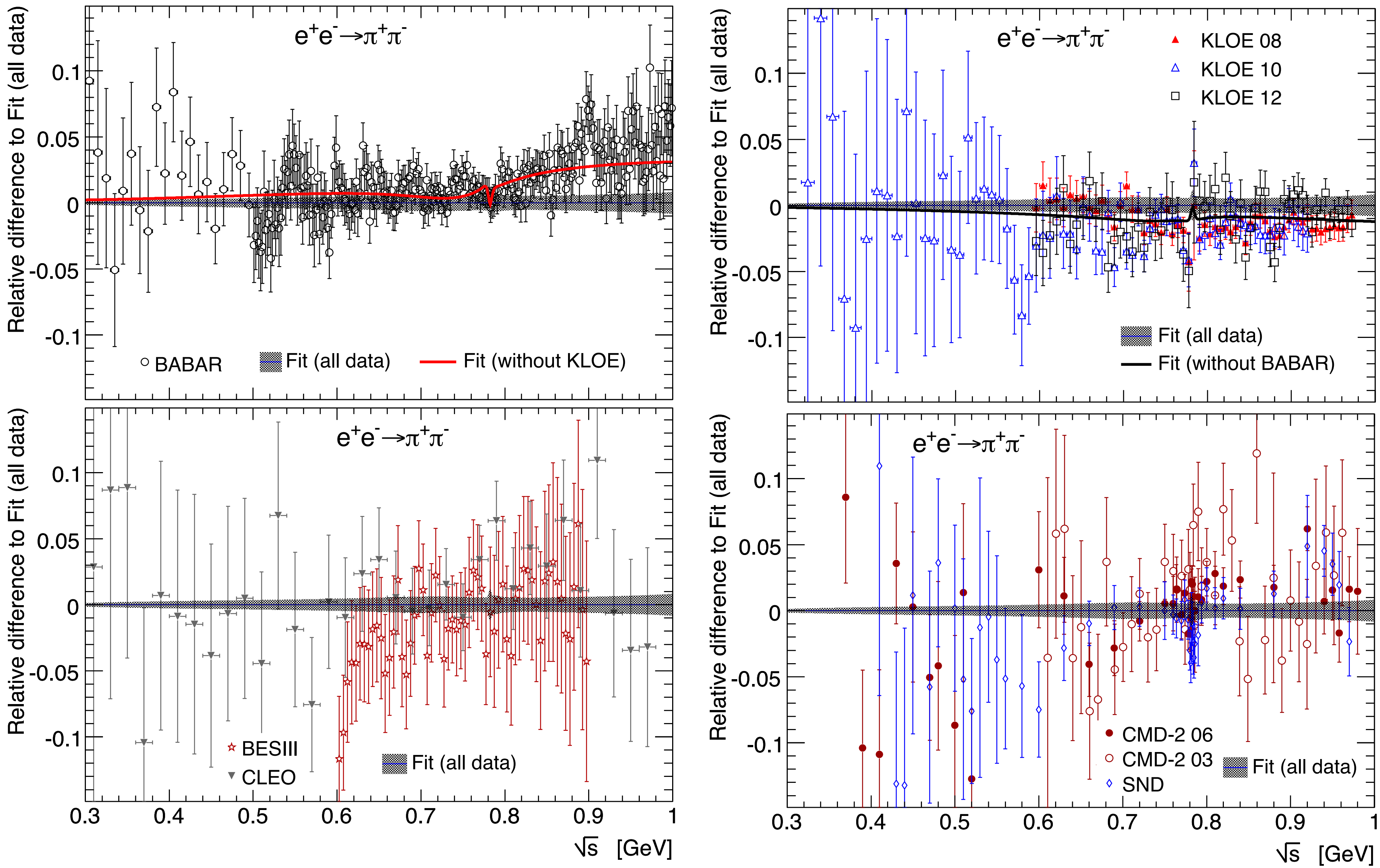

Comparison Fit and Data Integration

Figure from DHMZ, EPJC80 (2020) 241

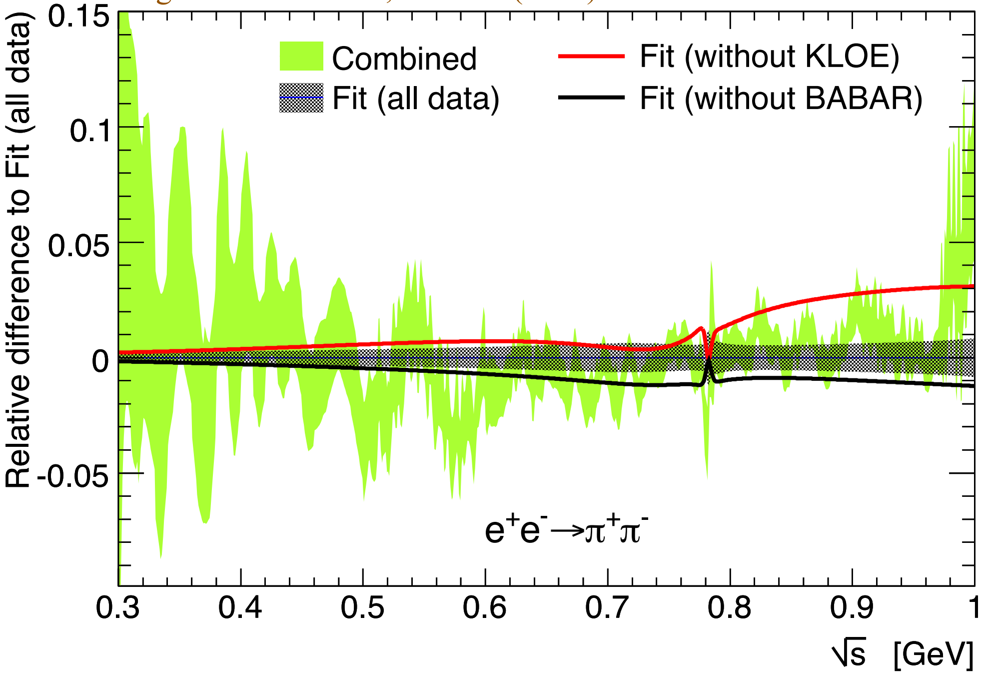

- ❒ Use fit only below 0.6 GeV for a_μ^{had} integral
  - ➤ Where the data are less precise and scarce
  - ➤ Less affected by potential uncertainties of inelastic contribution at high energy

$\sqrt{s}$ range [GeV]	a_μ^{had} $[10^{-10}]$ Fit	a_μ^{had} $[10^{-10}]$ Data Integration
0.3 - 0.6	$109.8 \pm 0.4_{exp} \pm 0.4_{para*}$	$109.6 \pm 1.0_{exp}$

⇒ The difference 0.2 ± 0.8 (correlation accounted for)

⇒ The fit improves the precision by ~2

* Parameter uncertainty corresponds to variations by removing the B_1 term in the phase shift formula and by varying $\sqrt{s_0}$ from 1.05 GeV to 1.3 GeV

Combined Results Fit [<0.6 GeV] + Data [0.6-1.8 GeV]

Take into account the correlation of 62% (based on pseudo-data samples) of the two regions

$\sqrt{s}$ range [GeV]	a_μ^{had} [10^{-10}] All data	a_μ^{had} [10^{-10}] All but BABAR	a_μ^{had} [10^{-10}] All but KLOE
threshold - 1.8	$506.9 \pm 1.9_{total}$	$505.0 \pm 2.1_{total}$	$510.6 \pm 2.2_{total}$

⇒ The difference "All but BABAR" and "All but KLOE" = 5.6 to be compared with 1.9 uncertainty with "All data"

- ➤ The local error inflation is not sufficient to amplify the uncertainty
- ➤ Global tension (normalisation/shape) not previously accounted for
- ➤ Potential underestimated uncertainty in at least one of the measurements?
- ➤ Other measurements not precise enough and are in agreement with BABAR or KLOE

⇒ Given the fact we do not know which dataset is problematic, we decide to

- ➤ Add half of the discrepancy (2.8) as an additional uncertainty (correcting the local PDG inflation to avoid double counting)
- ➤ Take the mean value "All but BABAR" and "All but KLOE" as our central value

Three Pions Channel - 2nd Dominant Channel

DHMZ17

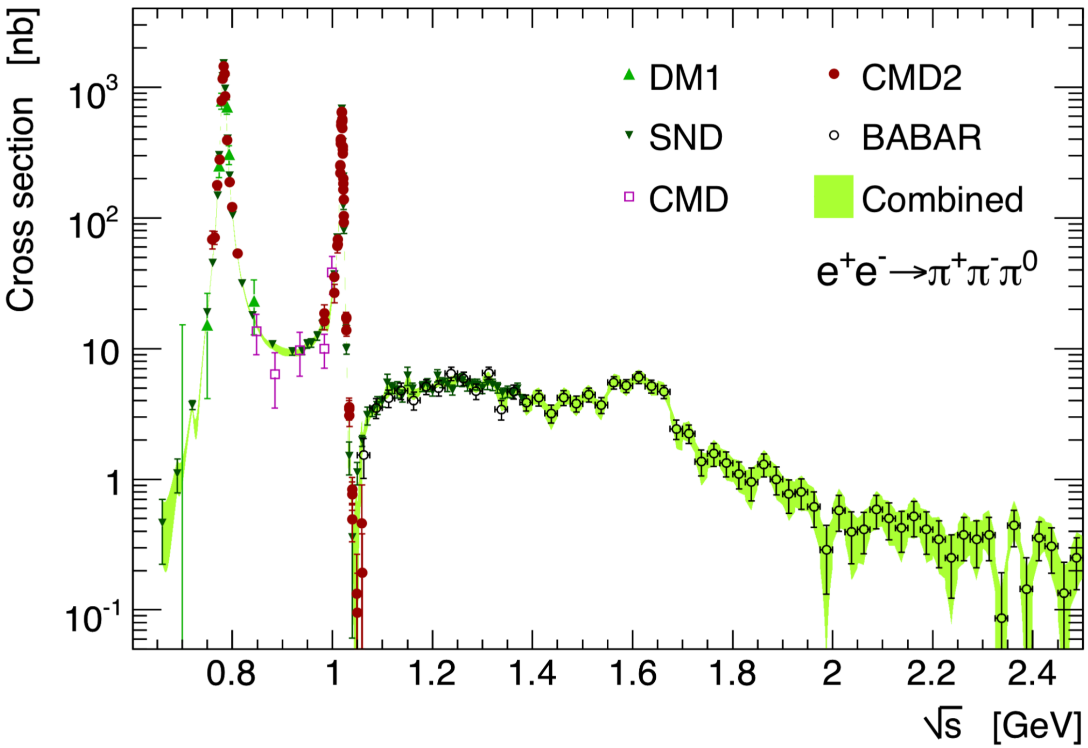

New Belle II measurement to be included in a future combination

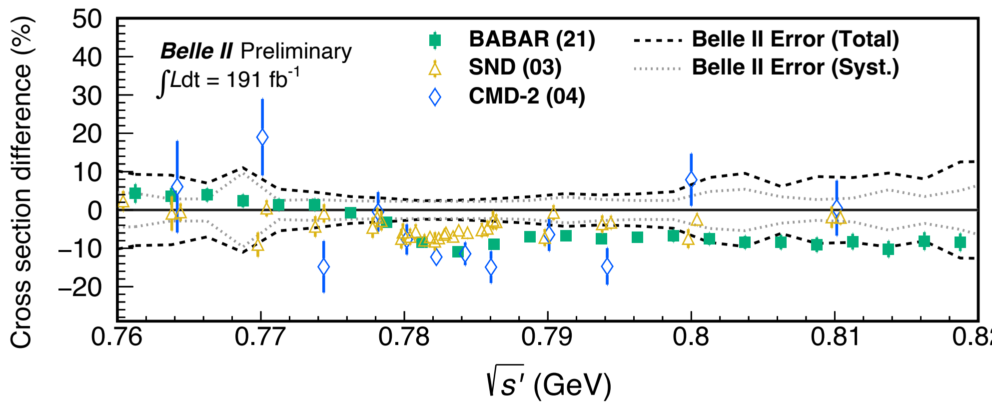

Comparison of 4π Channels - 3rd Dominant Channels

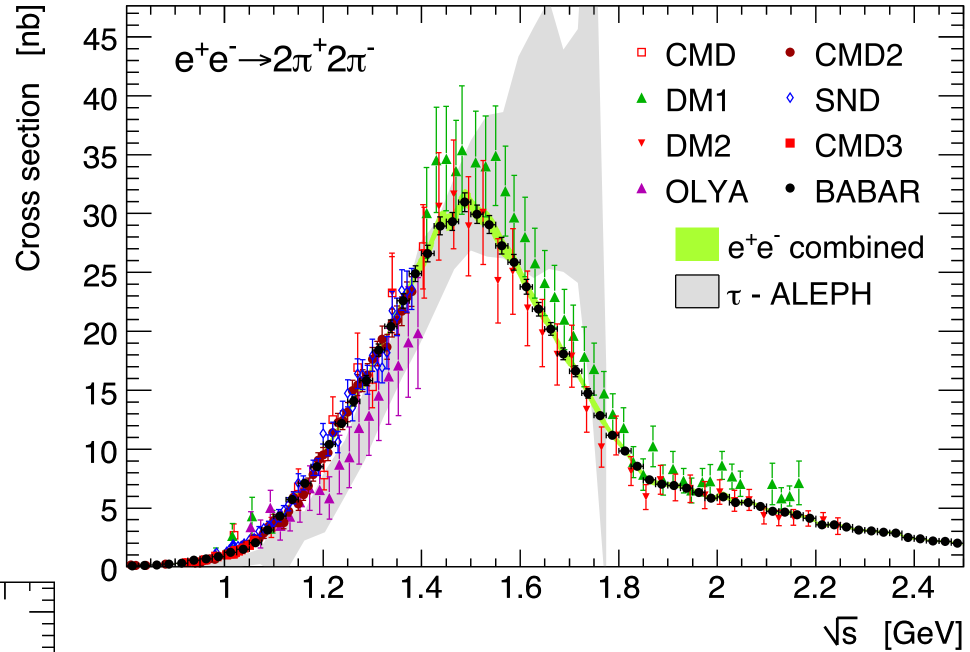

The precision of e⁺e⁻ data increased over time, a factor of 1.7-2.3 between 2011 and 2017

Figures from DHMZ17

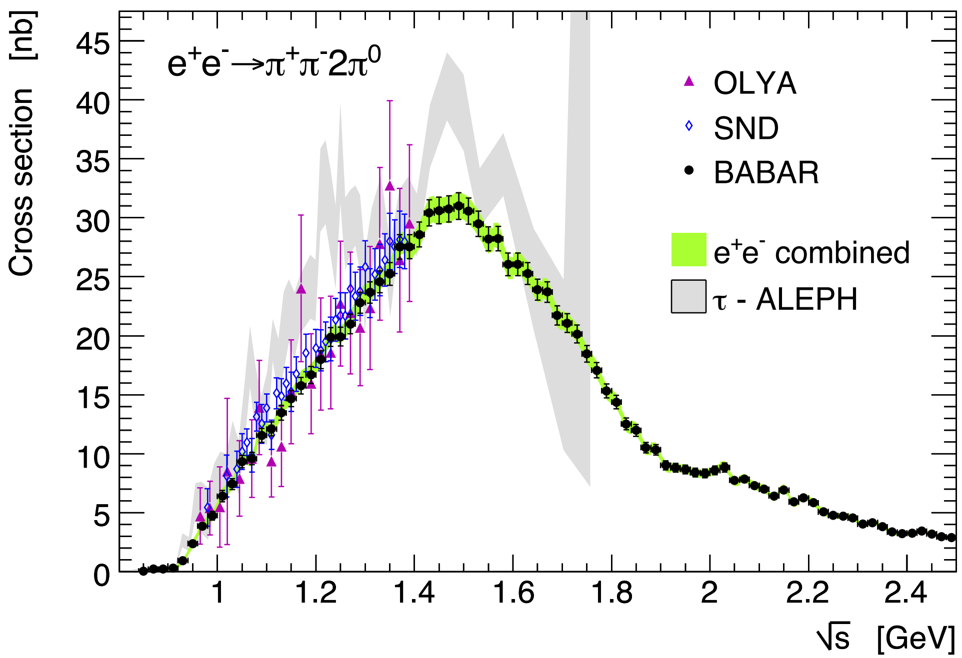

The less precise 4π τ data also shown

See slide 42 how tau data can be used

Tension in Other Channel (e.g. KK)

Figures from DHMZ19

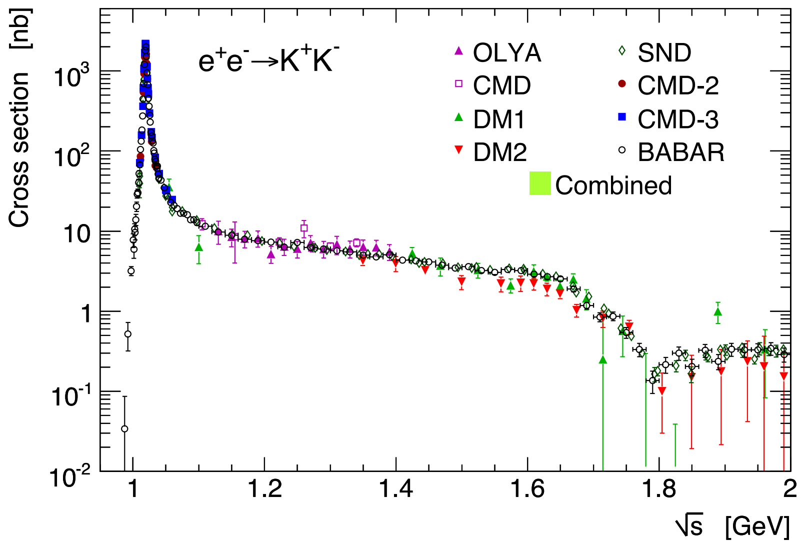

Several measurements with different precisions, CMD-2 and CMD-3 do not agree within the quoted uncertainties!
➜ Large error scaling factors
though this channel only contributes 3.3% to LO HVP and 1.2% to uncertainty-squared.

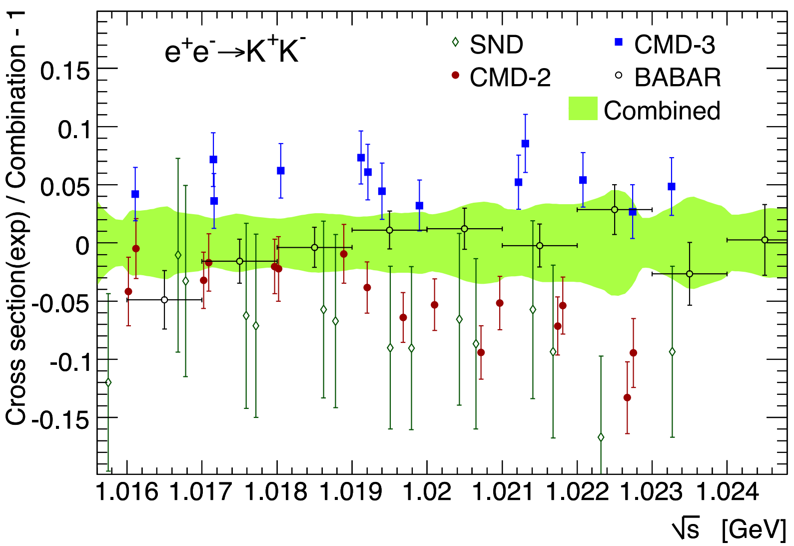

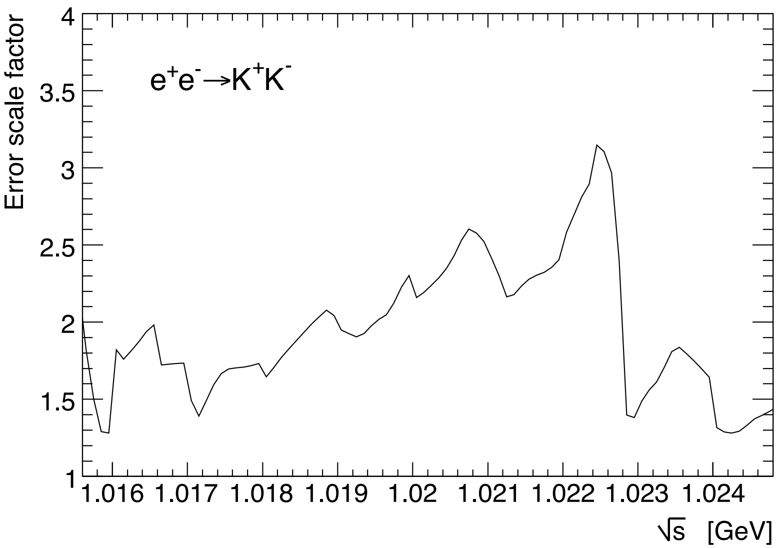

Other Channels e.g. Those Measured by BABAR

There are many exclusive channels (~ 40 processes) contributing to HVP

Here are some example measurements from BABAR

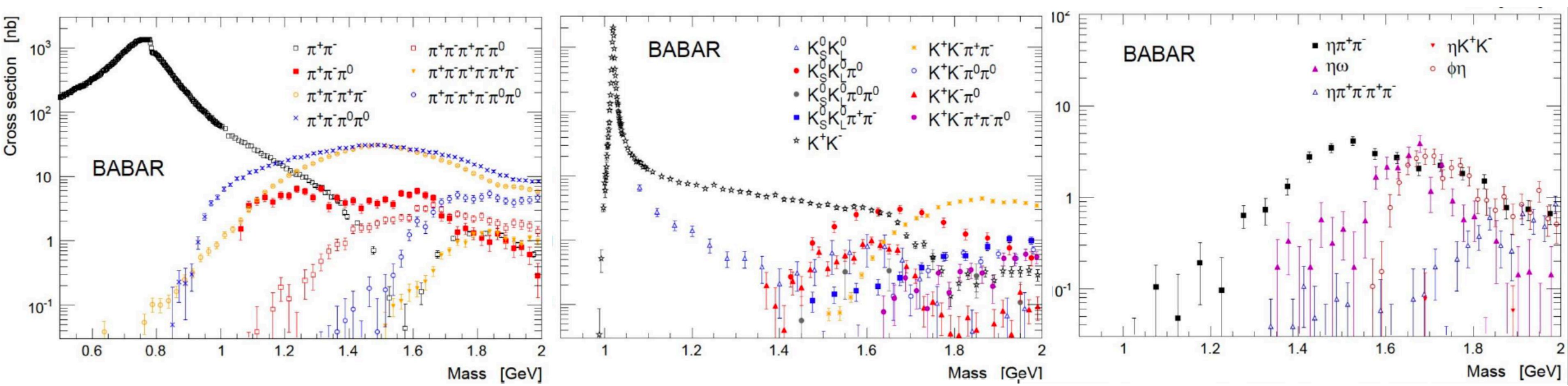

Many channels contribute up to 2 GeV and beyond

The evaluation of the exclusive channels is performed up to 1.8 GeV by DHMZ
Beyond 1.8 GeV, the evaluation is done with pQCD
Between 1.8 and 2 GeV, there is a possibility to compare the two, see slide 39

KKbar+π's Channels DHMZ17

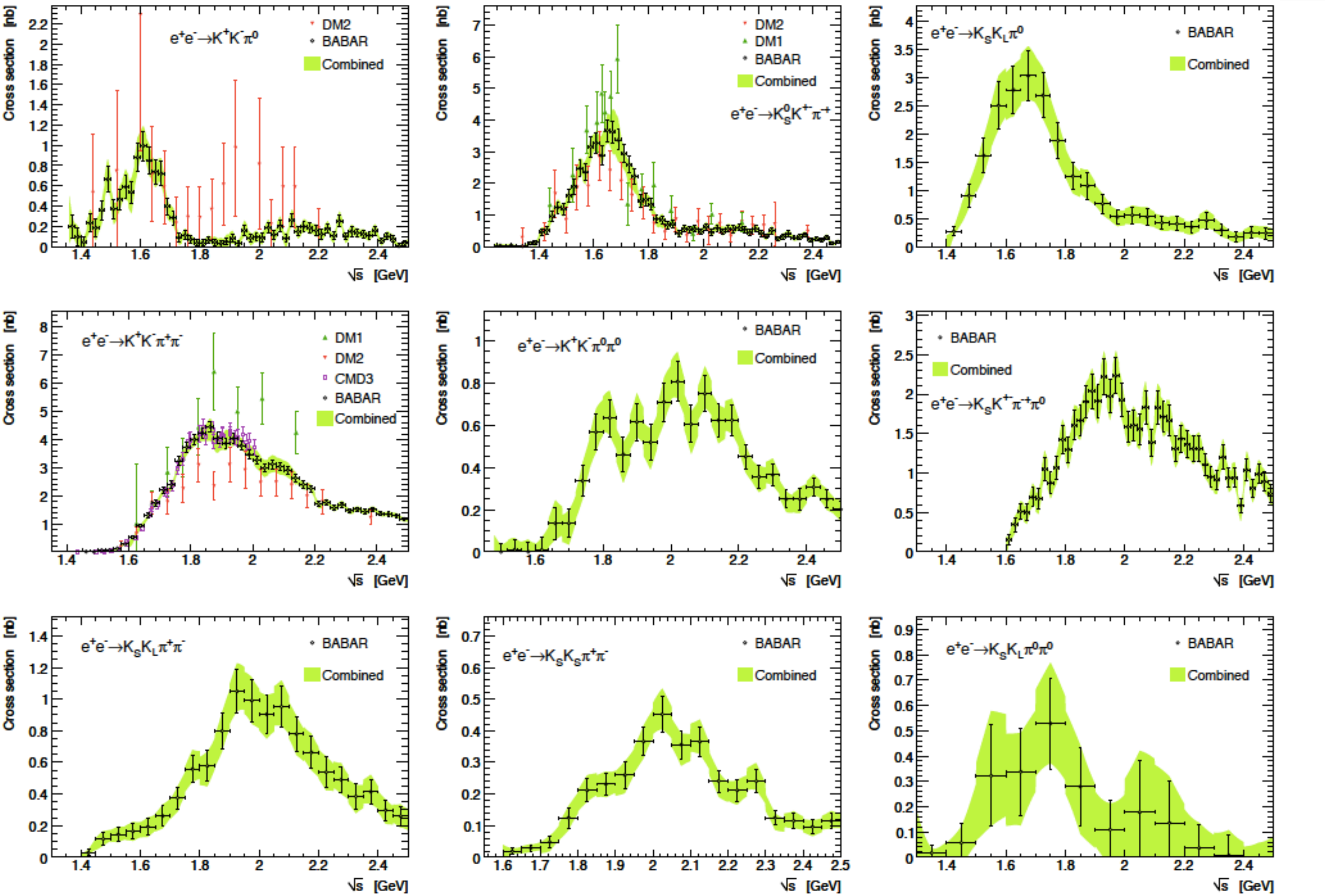

Contributions in the Region 1.8-3.7 GeV

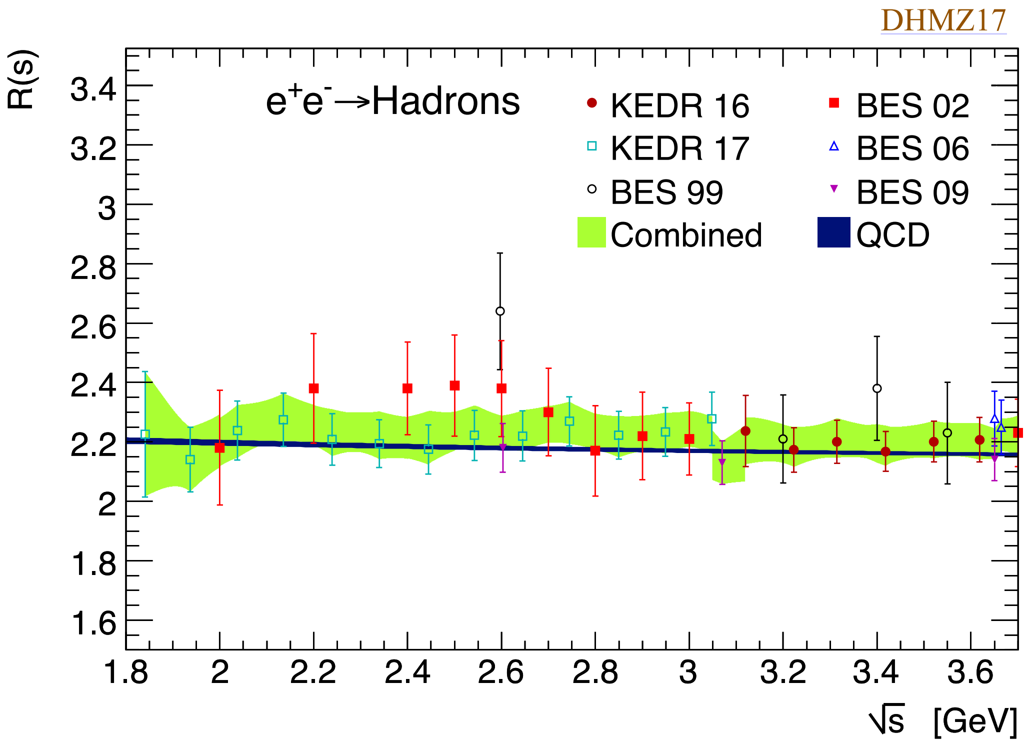

BES III results to be included: ~tension with pQCD and with KEDR 16

Energy range [GeV]	1.8 - 2.0 [2020]	2.0 - 3.7 [2017]
Data	7.65 ± 0.31	25.82 ± 0.61
pQCD	8.30 ± 0.09	25.15 ± 0.19
Difference	0.65 → dual	agree < 1σ

pQCD evaluated from 4 loops + $O(\alpha_s^2)$ quark mass corrections
Uncertainties: α_s, truncation, FOPT/CIPT, m_q

Contributions from Charm Resonance Region

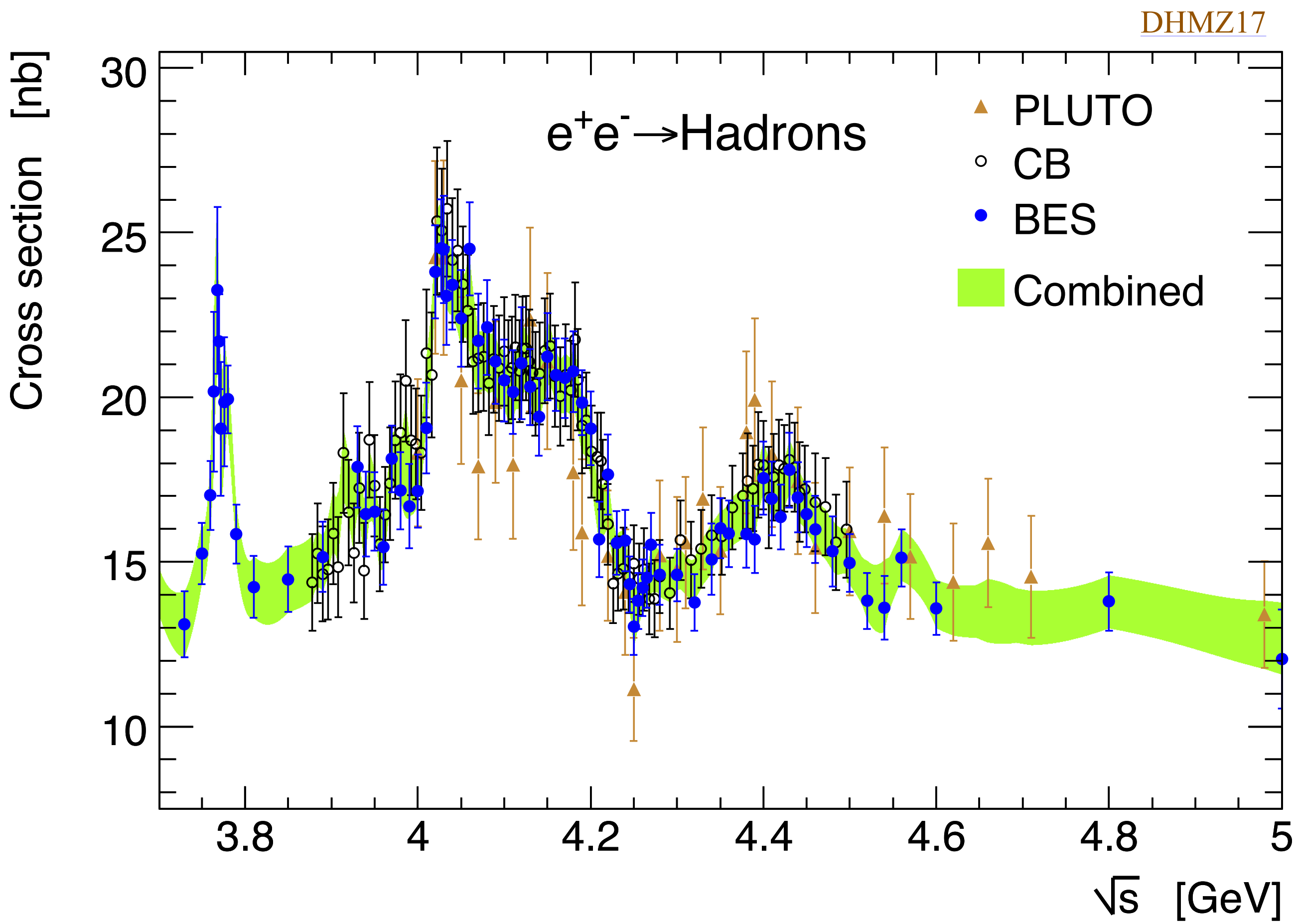

$7.29 \pm 0.05 \pm 0.30 \pm 0.00 \Rightarrow 1.05\%$ of $a_\mu^{\mathrm{had,\,LO}}$

stat sys cor

Overall Results

Channel	$a_\mu^{\text{had, LO}}[10^{-10}]$	$\Delta\alpha(m_Z^2)[10^{-4}]$
$\pi^0\gamma$	$4.29 \pm 0.06 \pm 0.04 \pm 0.07$	$0.35 \pm 0.00 \pm 0.00 \pm 0.01$
$\eta\gamma$	$0.65 \pm 0.02 \pm 0.01 \pm 0.01$	$0.08 \pm 0.00 \pm 0.00 \pm 0.00$
$\pi^+\pi^-$	$507.80 \pm 0.83 \pm 3.19 \pm 0.60$	$34.49 \pm 0.06 \pm 0.20 \pm 0.04$
$\pi^+\pi^-\pi^0$	$46.20 \pm 0.40 \pm 1.10 \pm 0.86$	$4.60 \pm 0.04 \pm 0.11 \pm 0.08$
$2\pi^+2\pi^-$	$13.68 \pm 0.03 \pm 0.27 \pm 0.14$	$3.58 \pm 0.01 \pm 0.07 \pm 0.03$
$\pi^+\pi^-2\pi^0$	$18.03 \pm 0.06 \pm 0.48 \pm 0.26$	$4.45 \pm 0.02 \pm 0.12 \pm 0.07$
$2\pi^+2\pi^-\pi^0$ (η excl.)	$0.69 \pm 0.04 \pm 0.06 \pm 0.03$	$0.21 \pm 0.01 \pm 0.02 \pm 0.01$
$\pi^+\pi^-3\pi^0$ (η excl.)	$0.49 \pm 0.03 \pm 0.09 \pm 0.00$	$0.15 \pm 0.01 \pm 0.03 \pm 0.00$
$3\pi^+3\pi^-$	$0.11 \pm 0.00 \pm 0.01 \pm 0.00$	$0.04 \pm 0.00 \pm 0.00 \pm 0.00$
$2\pi^+2\pi^-2\pi^0$ (η excl.)	$0.71 \pm 0.06 \pm 0.07 \pm 0.14$	$0.25 \pm 0.02 \pm 0.02 \pm 0.05$
$\pi^+\pi^-4\pi^0$ (η excl., isospin)	$0.08 \pm 0.01 \pm 0.08 \pm 0.00$	$0.03 \pm 0.00 \pm 0.03 \pm 0.00$
$\eta\pi^+\pi^-$	$1.19 \pm 0.02 \pm 0.04 \pm 0.02$	$0.35 \pm 0.01 \pm 0.01 \pm 0.01$
$\eta\omega$	$0.35 \pm 0.01 \pm 0.02 \pm 0.01$	$0.11 \pm 0.00 \pm 0.01 \pm 0.00$
$\eta\pi^+\pi^-\pi^0$(non-ω,ϕ)	$0.34 \pm 0.03 \pm 0.03 \pm 0.04$	$0.12 \pm 0.01 \pm 0.01 \pm 0.01$
$\eta 2\pi^+2\pi^-$	$0.02 \pm 0.01 \pm 0.00 \pm 0.00$	$0.01 \pm 0.00 \pm 0.00 \pm 0.00$
$\omega\eta\pi^0$	$0.06 \pm 0.01 \pm 0.01 \pm 0.00$	$0.02 \pm 0.00 \pm 0.00 \pm 0.00$
$\omega\pi^0$ ($\omega \to \pi^0\gamma$)	$0.94 \pm 0.01 \pm 0.03 \pm 0.00$	$0.20 \pm 0.00 \pm 0.01 \pm 0.00$
$\omega(\pi\pi)^0$ ($\omega \to \pi^0\gamma$)	$0.07 \pm 0.00 \pm 0.00 \pm 0.00$	$0.02 \pm 0.00 \pm 0.00 \pm 0.00$
ω (non-$3\pi, \pi\gamma, \eta\gamma$)	$0.04 \pm 0.00 \pm 0.00 \pm 0.00$	$0.00 \pm 0.00 \pm 0.00 \pm 0.00$
K^+K^-	$23.08 \pm 0.20 \pm 0.33 \pm 0.21$	$3.35 \pm 0.03 \pm 0.05 \pm 0.03$
$K_S K_L$	$12.82 \pm 0.06 \pm 0.18 \pm 0.15$	$1.74 \pm 0.01 \pm 0.03 \pm 0.02$
ϕ (non-$K\overline{K}, 3\pi, \pi\gamma, \eta\gamma$)	$0.05 \pm 0.00 \pm 0.00 \pm 0.00$	$0.01 \pm 0.00 \pm 0.00 \pm 0.00$
$K\overline{K}\pi$	$2.45 \pm 0.05 \pm 0.10 \pm 0.06$	$0.78 \pm 0.02 \pm 0.03 \pm 0.02$
$K\overline{K}2\pi$	$0.85 \pm 0.02 \pm 0.05 \pm 0.01$	$0.30 \pm 0.01 \pm 0.02 \pm 0.00$
$K\overline{K}3\pi$ (estimate)	$-0.02 \pm 0.01 \pm 0.01 \pm 0.00$	$-0.01 \pm 0.00 \pm 0.00 \pm 0.00$
$\eta\phi$	$0.33 \pm 0.01 \pm 0.01 \pm 0.00$	$0.11 \pm 0.00 \pm 0.00 \pm 0.00$
$\eta K\overline{K}$ (non-ϕ)	$0.01 \pm 0.01 \pm 0.01 \pm 0.00$	$0.00 \pm 0.00 \pm 0.01 \pm 0.00$
$\omega K\overline{K}$ ($\omega \to \pi^0\gamma$)	$0.01 \pm 0.00 \pm 0.00 \pm 0.00$	$0.00 \pm 0.00 \pm 0.00 \pm 0.00$
$\omega 3\pi$ ($\omega \to \pi^0\gamma$)	$0.06 \pm 0.01 \pm 0.01 \pm 0.01$	$0.02 \pm 0.00 \pm 0.00 \pm 0.00$
7π ($3\pi^+3\pi^-\pi^0$ + estimate)	$0.02 \pm 0.00 \pm 0.01 \pm 0.00$	$0.01 \pm 0.00 \pm 0.00 \pm 0.00$
J/ψ (BW integral)	6.28 ± 0.07	7.09 ± 0.08
$\psi(2S)$ (BW integral)	1.57 ± 0.03	2.50 ± 0.04
R data [3.7 − 5.0] GeV	$7.29 \pm 0.05 \pm 0.30 \pm 0.00$	$15.79 \pm 0.12 \pm 0.66 \pm 0.00$
R_{QCD} $[1.8 - 3.7\ \text{GeV}]_{uds}$	$33.45 \pm 0.28 \pm 0.65_{\text{dual}}$	$24.27 \pm 0.18 \pm 0.28_{\text{dual}}$
R_{QCD} $[5.0 - 9.3\ \text{GeV}]_{udsc}$	6.86 ± 0.04	34.89 ± 0.17
R_{QCD} $[9.3 - 12.0\ \text{GeV}]_{udscb}$	1.21 ± 0.01	15.56 ± 0.04
R_{QCD} $[12.0 - 40.0\ \text{GeV}]_{udscb}$	1.64 ± 0.00	77.94 ± 0.12
R_{QCD} $[> 40.0\ \text{GeV}]_{udscb}$	0.16 ± 0.00	42.70 ± 0.06
R_{QCD} $[> 40.0\ \text{GeV}]_{t}$	0.00 ± 0.00	-0.72 ± 0.01
Sum	$693.9 \pm 1.0 \pm 3.4 \pm 1.6 \pm 0.1_\psi \pm 0.7_{\text{QCD}}$	$275.42 \pm 0.15 \pm 0.72 \pm 0.23 \pm 0.09_\psi \pm 0.55_{\text{QCD}}$

Table taken from DHMZ, EPJC80 (2020) 241

An Alternative Way Used to Evaluate HVP

Proposed by Alemany-Davier-Hoecker, EPJC 2 (1998) 123

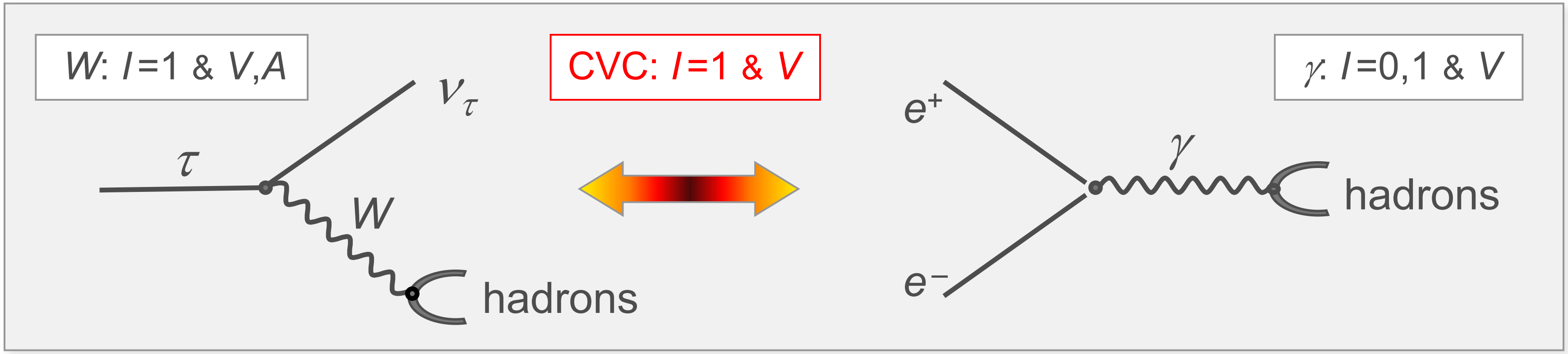

Hadronic physics factorises in Spectral Functions:
Isospin symmetry connects I=1 e^+e^- cross section to vector τ spectral functions

Fundamental ingredient relating long distance (resonances) to short distance description (QCD)

$$\sigma^{(I=1)}\left[e^+e^- \to \pi^+\pi^-\right] = \frac{4\pi\alpha^2}{s}\upsilon\left[\tau^- \to \pi^-\pi^0\nu_\tau\right]$$

$$\upsilon\left[\tau^- \to \pi^-\pi^0\nu_\tau\right] \propto \frac{\mathrm{BR}\left[\tau^- \to \pi^-\pi^0\nu_\tau\right]}{\mathrm{BR}\left[\tau^- \to e^-\bar{\nu}_e\nu_\tau\right]} \frac{1}{N_{\pi\pi^0}}\frac{dN_{\pi\pi^0}}{ds} \frac{m_\tau^2}{\left(1-s/m_\tau^2\right)^2\left(1+s/m_\tau^2\right)}$$

Branching fractions | Mass spectrum | Kinematic factors (PS)

Known Isospin Breaking Corrections

Davier et al., EPJC66 (2010) 127

$$v_{1,X^-}(s) = \frac{m_\tau^2}{6|V_{ud}|^2}\frac{\mathcal{B}_{X^-}}{\mathcal{B}_e}\frac{1}{N_X}\frac{dN_X}{ds} \times \left(1-\frac{s}{m_\tau^2}\right)^{-2}\left(1+\frac{2s}{m_\tau^2}\right)^{-1}\frac{R_{\rm IB}(s)}{S_{\rm EW}},$$

$$R_{\rm IB}(s) = \frac{{\rm FSR}(s)}{G_{\rm EM}(s)}\frac{\beta_0^3(s)}{\beta_-^3(s)}\left|\frac{F_0(s)}{F_-(s)}\right|^2$$

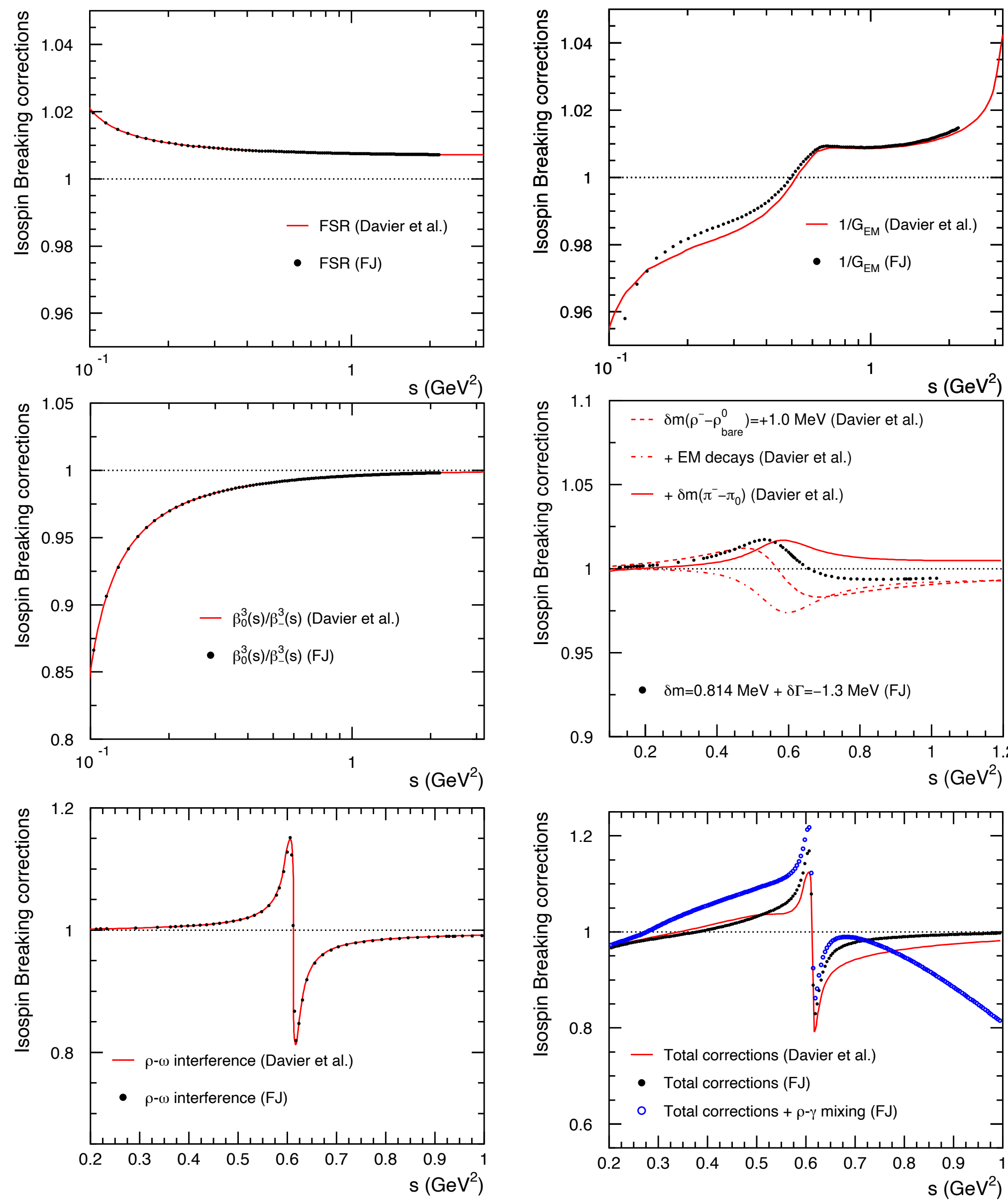

Good agreement between Davier et al. and FJ for most of the isospin breaking components

Figure 19 from WP20 (except for the middle-right plot)
Studies initiated by Davier et al., EPJC66 (2010) 127

Open Issue in 2π Channel

Take into account all known isospin breaking corrections except for the ρ–γ mixing correction

DHMYZ, EPJC66 (2010) 1

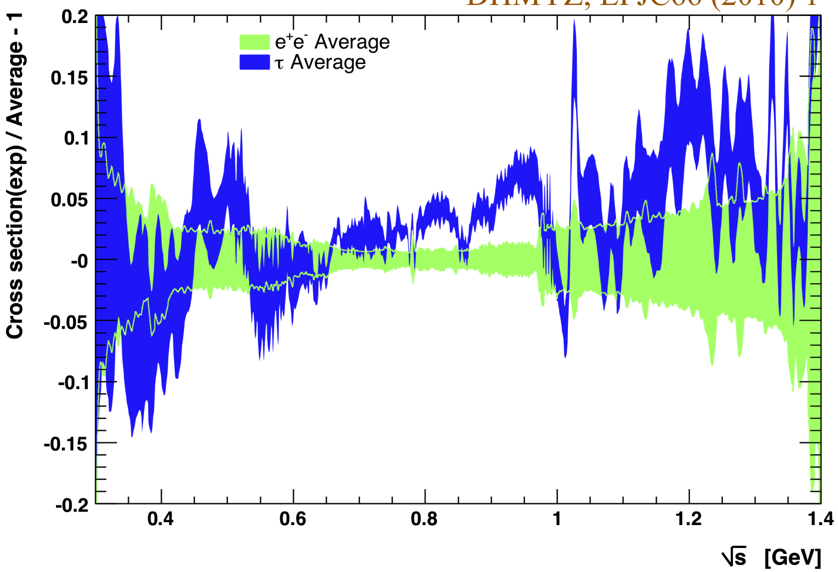

Modified version from Davier et al,, EPJC66 (2010) 127

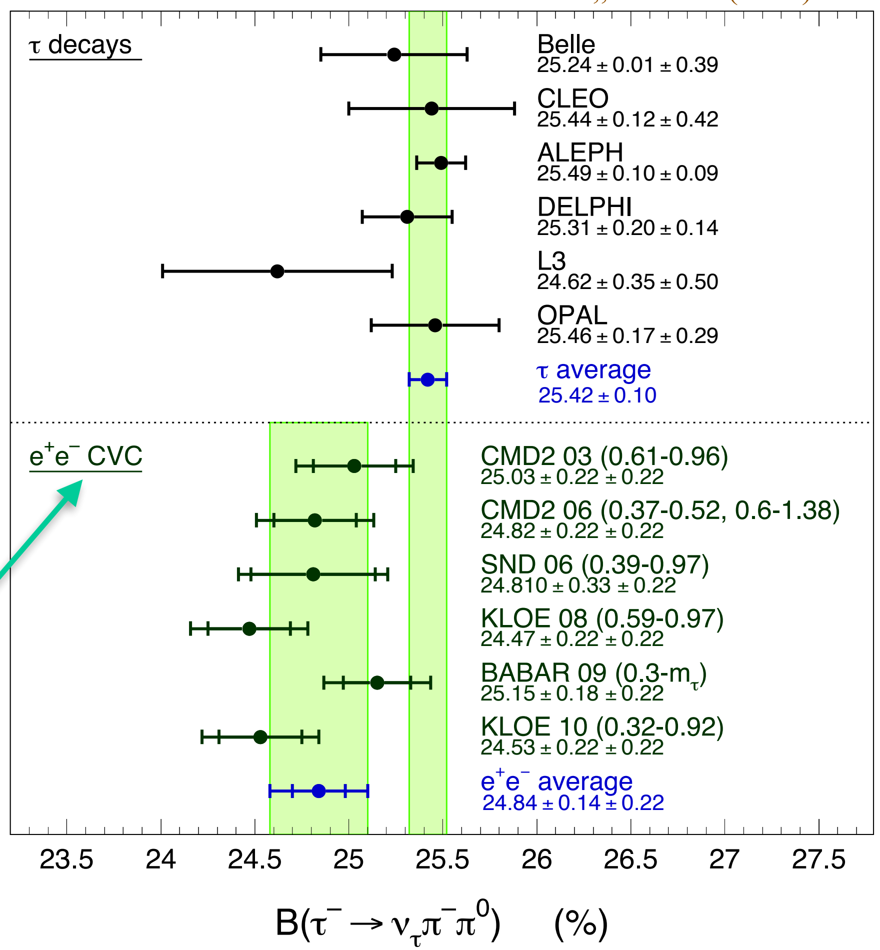

$$\mathcal{B}_X^{\mathrm{CVC}} = \frac{3}{2}\frac{\mathcal{B}_e|V_{ud}|^2}{\pi\alpha^2 m_\tau^2}\int_{s_{\min}}^{m_\tau^2} ds\, s\, \sigma_{X^0}^I \left(1-\frac{s}{m_\tau^2}\right)^2\left(1+\frac{2s}{m_\tau^2}\right)$$

Clear difference in shape and in BR
between e^+e^- and τ average (the picture will change if include CMD-3 but without KLOE)

DHMZ versus KNT Combination Procedures

Analysis aspect	DHMZ	KNT
Blinding	Not necessary (No ad-hoc choices to make)	Included for upcoming update
Binning	Fine (≤ 1 MeV) final binning for average and integrals. Large (O(100 MeV) or less) common binning @ intermediate step: compare statistics of experiments coherently for deriving weights in fine bins	Re-bin data into "clusters". Scans over cluster configurations for optimisation
Closure test	Using model for spectrum: negligible bias (since 2009)	Not performed
Additional constraints	Analyticity constraints for 2π channel	None
Fitting	χ^2 minimisation with correlated uncertainties incorporated locally (in fine & large bins), for deriving weights Full propagation of uncertainties & correlations	χ^2 minimisation with correlated uncertainties incorporated globally
Integration / interpolation	Av. of quadratic splines (3rd order polynomial), integral preservation in bins of measurements Analyticity-based function for 2π (< 0.6 GeV).	Trapezoidal for continuum, quintic for resonances
Uncertainty inflation	Local χ^2 uncertainty inflation (since 2009) Extra BABAR-KLOE systematic (since 2019)	Local χ^2 uncertainty inflation (adopted since 2017)
Inter-channel correlations	Taken into account (since 2010)	Not included
Missing channels	Estimated based on isospin symmetry (since 1997 ADH)	Adopted in subsequent updates

DHMZ versus KNT Combination Procedures

DHMZ:

- ➢ χ^2 computed locally (in each fine bin), taking into account correlations between measurements
- ➢ Used to determine the weights on the measurements in the combination and their level of agreement
- ➢ Uncertainties and correlations propagated using pseudo-experiments or ±1σ shifts of each uncertainty component

KNT:

- ➢ χ^2 computed globally (for full mass range)

$$\chi_I^2 = \sum_{i=1}^{N_{\text{tot}}} \sum_{j=1}^{N_{\text{tot}}} \left(R_i^{(m)} - \mathcal{R}_m^{i,I}\right) \mathbf{C}_I^{-1}\left(i^{(m)}, j^{(n)}\right)\left(R_j^{(n)} - \mathcal{R}_n^{j,I}\right)$$

KNT (1802.02995)

$$\chi^2 = \sum_{i=1}^{195} \sum_{j=1}^{195} \left(\sigma^0_{\pi\pi(\gamma)}(i) - \bar{\sigma}^0_{\pi\pi(\gamma)}(m)\right) \mathbf{C}^{-1}\left(i^{(m)}, j^{(n)}\right)\left(\sigma^0_{\pi\pi(\gamma)}(j) - \bar{\sigma}^0_{\pi\pi(\gamma)}(n)\right)$$

KLOE-KMT (1711.03085)

- ➢ relies on description of correlations on long ranges
- ➢ One of the main sources of differences for the uncertainty on a_μ

DHMZ vs KNT: Combing 3 KLOE Measurements

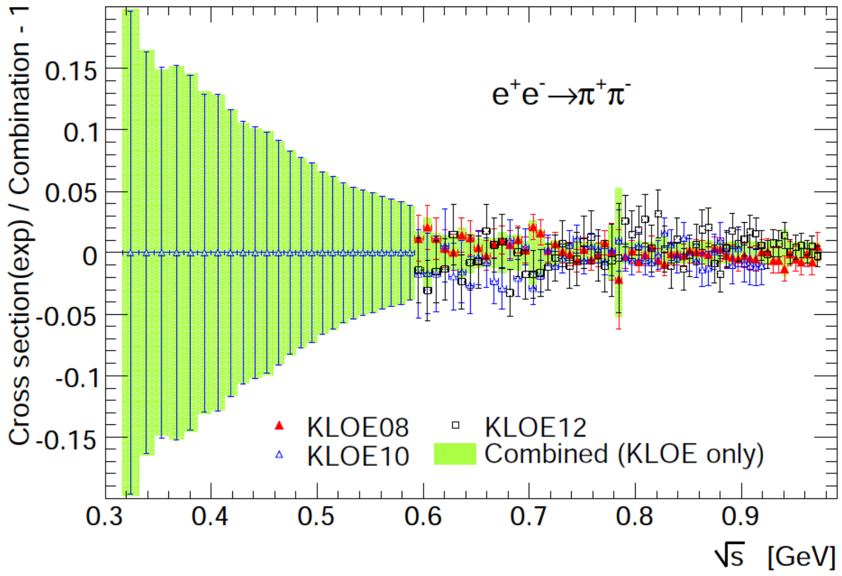

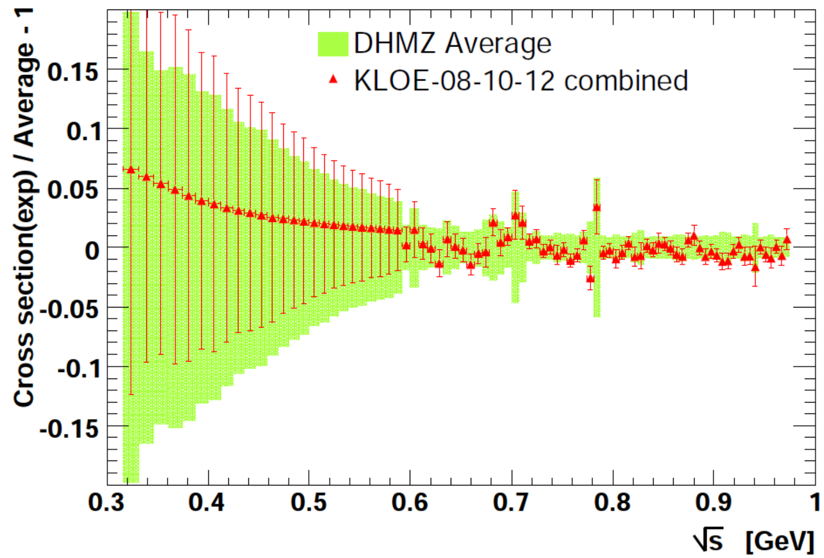

Local combination (DHMZ)

Information propagated between mass regions, through shifts of systematics - relying on correlations, amplitudes and shapes of systematics (KLOE-KT)

Combining 3 KLOE Measurements - Comparison

- Individual measurements:
  KLOE08 a_μ[0.6 ; 0.9] : 368.3 ± 3.2 [10^{-10}]
  KLOE10 a_μ[0.6 ; 0.9] : 365.6 ± 3.3
  KLOE12 a_μ[0.6 ; 0.9] : 366.8 ± 2.5

- Correlation matrix:

	08	10	12
08	1	0.70	0.35
10	0.70	1	0.19
12	0.35	0.19	1

  Amount of independent information provided by each measurement

- KLOE-08-10-12(DHMZ) - a_μ[0.6 ; 0.9] : 366.5 ± 2.8 (without χ^2 rescaling: ± 2.2)
  ➔ Conservative treatment of uncertainties and correlations (*not perfectly known*) in weight determination

- KLOE-08-10-12(KLOE-KT) - a_μ[0.6 ; 0.9]GeV : 366.9 ± 2.2 (includes χ^2 rescaling)
  Assuming perfect knowledge of the correlations to minimise average uncertainty

DHMZ versus KNT: Selected Channels

WP20: Phys. Rep. 887 (2020) 1

	DHMZ19	KNT19	Difference
$\pi^+\pi^-$	507.85(0.83)(3.23)(0.55)	504.23(1.90)	3.62
$\pi^+\pi^-\pi^0$	46.21(0.40)(1.10)(0.86)	46.63(94)	−0.42
$\pi^+\pi^-\pi^+\pi^-$	13.68(0.03)(0.27)(0.14)	13.99(19)	−0.31
$\pi^+\pi^-\pi^0\pi^0$	18.03(0.06)(0.48)(0.26)	18.15(74)	−0.12
K^+K^-	23.08(0.20)(0.33)(0.21)	23.00(22)	0.08
K_SK_L	12.82(0.06)(0.18)(0.15)	13.04(19)	−0.22
$\pi^0\gamma$	4.41(0.06)(0.04)(0.07)	4.58(10)	−0.17
Sum of the above	626.08(0.95)(3.48)(1.47)	623.62(2.27)	2.46
[1.8, 3.7] GeV (without $c\bar{c}$)	33.45(71)	34.45(56)	−1.00
J/ψ, $\psi(2S)$	7.76(12)	7.84(19)	−0.08
[3.7, ∞) GeV	17.15(31)	16.95(19)	0.20
Total $a_\mu^{\mathrm{HVP,\ LO}}$	$694.0(1.0)(3.5)(1.6)(0.1)_\psi(0.7)_{\mathrm{DV+QCD}}$	692.8(2.4)	1.2

Large difference in 2π compensated by other channels

Study of Higher Order Radiations from BABAR

Motivated by
- the current discrepancy between KLOE and BABAR
- Both used NLO Phokhara event generator

BABAR23

BABAR measured higher order radiations using its full data samples by performing

- ➢ Two NLO fits
  - ➢ Small Angle (SA) fit
  - ➢ Large Angle (LA) fit
- ➢ Three NNLO fits
  - ➢ 2SA fit
  - ➢ SA+LA fit
  - ➢ 2LA fits

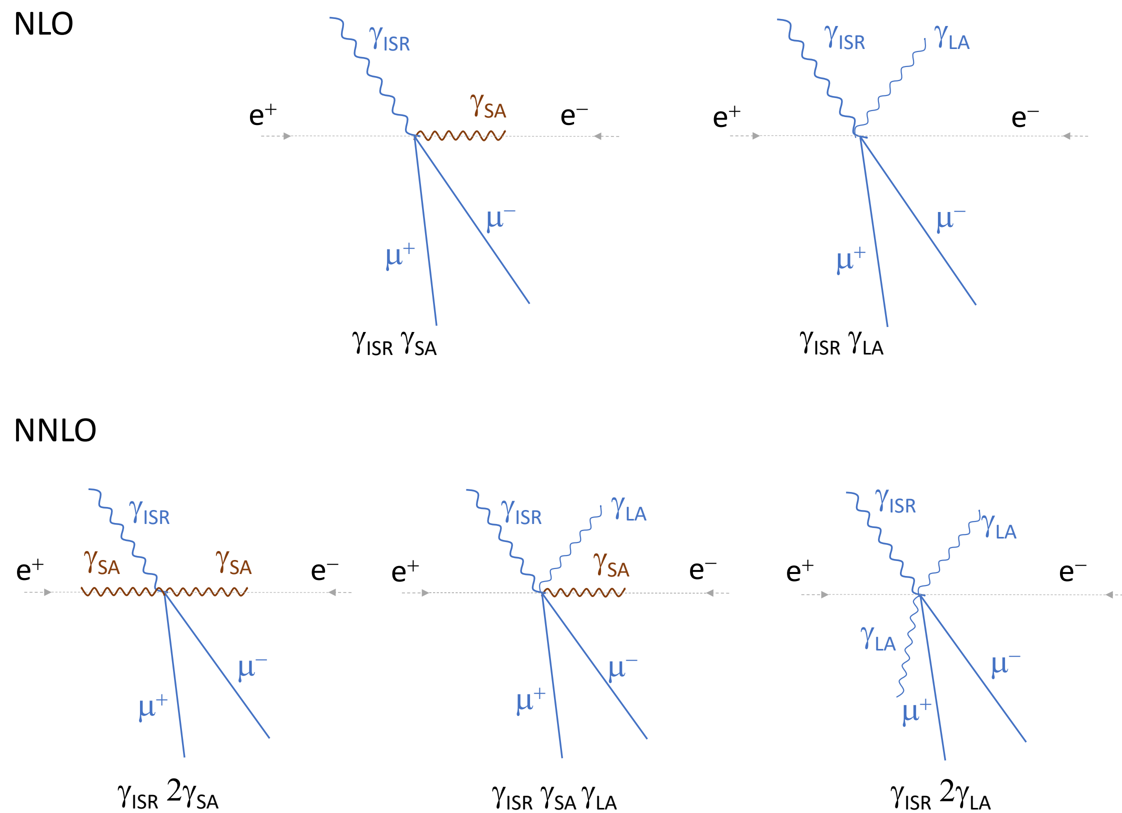

Two Key Observations of BABAR

BABAR23

Key observation number 1:

➢ The sum of NNLO categories for photon energy threshold > 100-200 MeV is ~3.5%

Key observation number 2:

➢ Phokhara prediction for NLO small-angle photons is too higher by ~25%

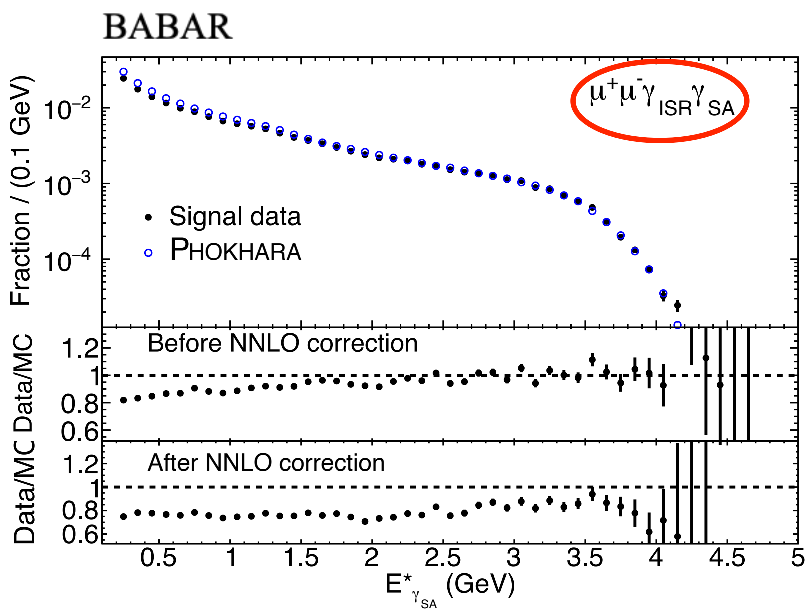

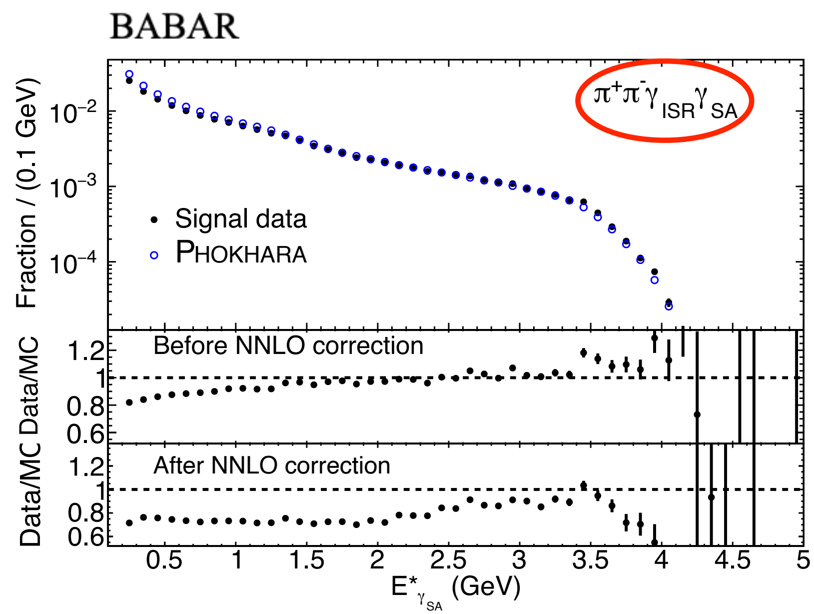

Consequences of BABAR's Results

- BABAR analysis performed with loose selections, efficiencies obtained with data
  - ➔ The effect of missing NNLO and NLO excess in Phokhara on acceptance (0.03±0.01)% well below the quoted syst. uncertainty
- Using fast simulations, studied possible effects for the KLOE and BESIII analyses
  - ➔ Found larger effects beyond the quoted uncertainty of 0.5%
  - ➔ Real effects can only be accessed by the KLOE and BESIII themselves

DHLMZ23

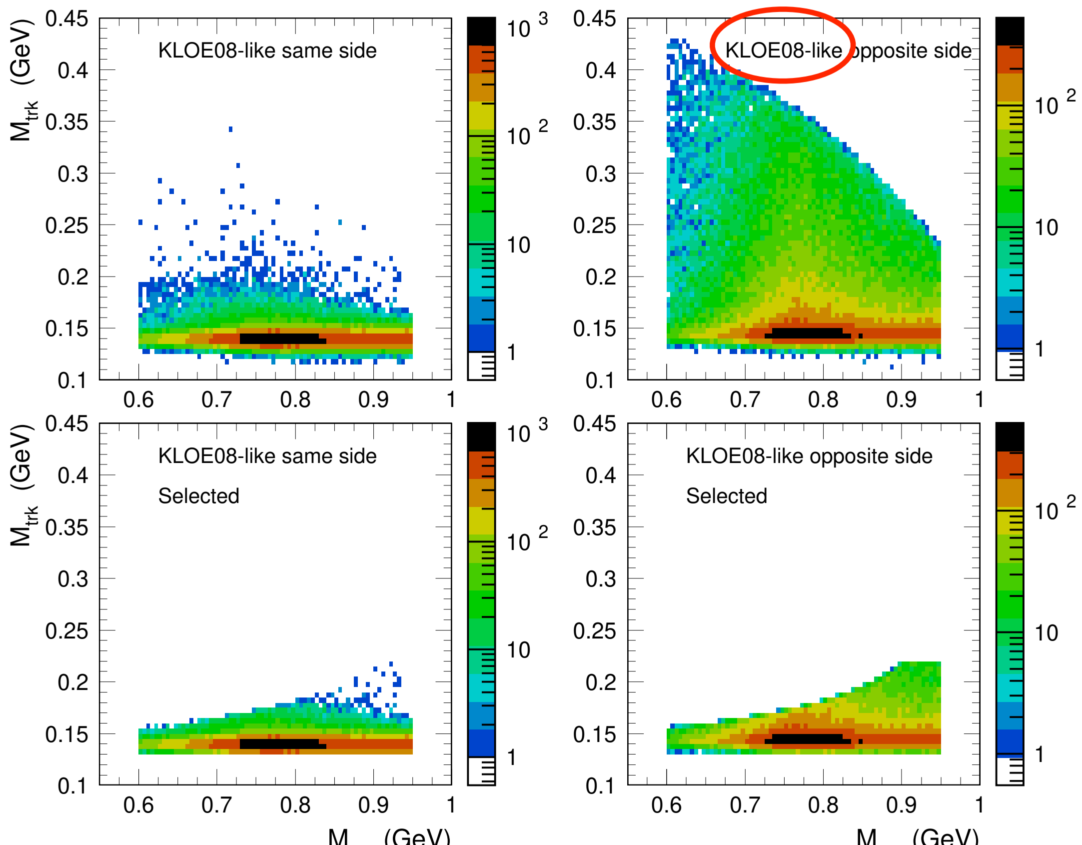

KLOE and BESIII do not study additional photons and rely on Phokhara for radiative corrections

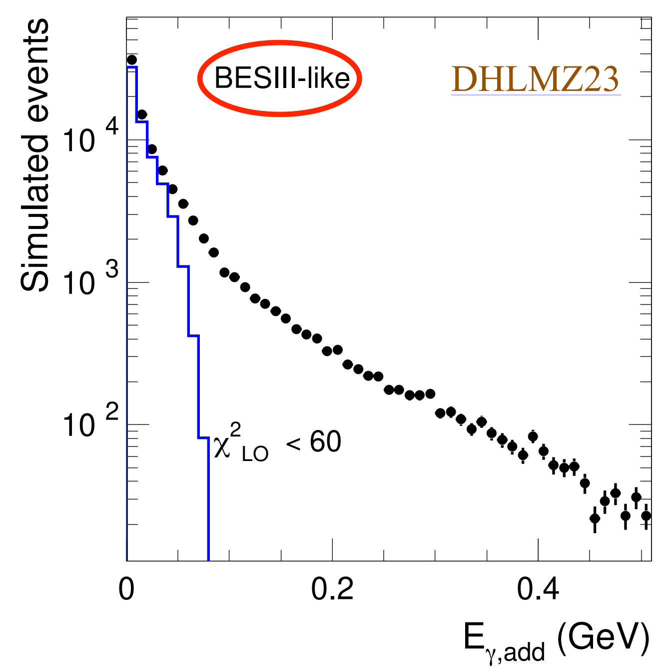

New Landscape of the Driven-Driven Prediction

DHLMZ23

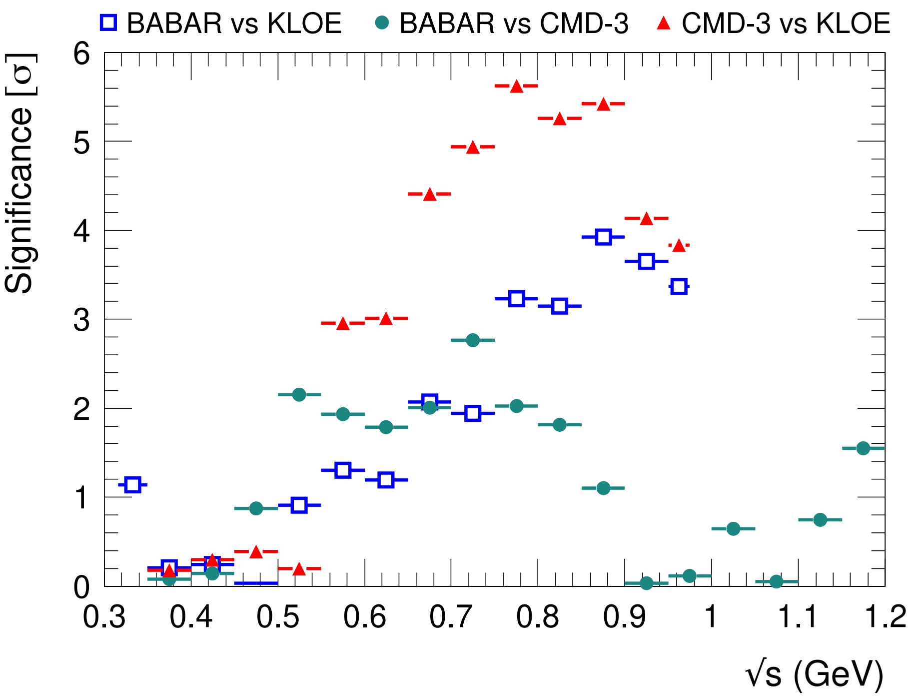

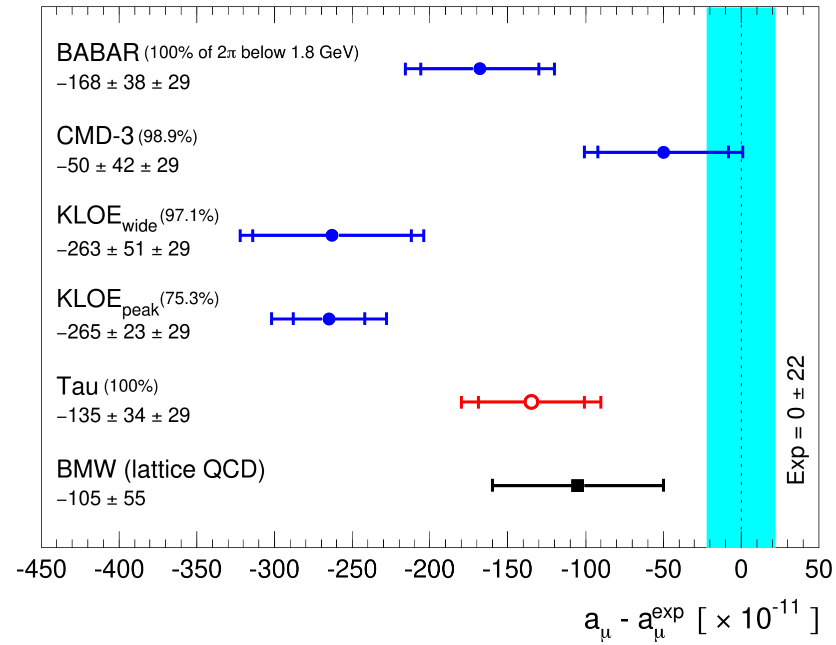

- ➢ BABAR and CMD-3 in agreement within 3σ in the full mass range
- ➢ KLOE and CMS-3 have the largest discrepancy, over 5σ in the dominant rho peak region
- ➢ BABAR, CMD-3 and tau are consistent and also in agreement with BMW (lattice prediction)

Summary and Perspectives

- The precision of the data-driven LO HVP prediction depends directly on the input data precision

- It depends to some extent also on the data combination strategy and uncertainty treatment

- There are significant discrepancies between measurements from different experiments
  - Need independent and high precision measurements including tau decays to clarify the situation
  - Need to understand the discrepancy between CMD-3 and CMD-2
  - Need to know if the existing measurements are affected by the deficiencies of the Phokhara MC event generator

- Need higher order MC generators in particular for those experiments relying on MC for higher order corrections

- The whole discussion applies also to the HVP contribution to the running QED coupling except that the QED kernel has a different energy dependence such that the data at higher energy plays a relatively more important role
  - Here the precision is important for the global EW fits